Warsaw University of Technology

FACULTY OF PHYSICS

Master's diploma thesis

in the field of study Applied Physics
and specialisation Nuclear Physics and Technology

Properties of quantum droplets at finite temperature

Mateusz Kowalczyk
student record book number 291543

thesis supervisors
dr hab. Krzysztof Pawłowski
dr Marek Tylutki

WARSAW 2022

Properties of quantum droplets at finite temperature

We investigate a one-dimensional, strongly-interacting Bose system with an additional non-local dipolar term. Such a system offers a new form of ultra dilute state of matter – quantum droplet. This new quantum state may arise when in an ultracold system, one has two types of interactions with different nature – attractive and repulsive. There may occur a situation when the mean-field terms describing the competing forces are close to zero, and the significant role plays quantum corrections. The formation of a quantum droplet is possible in both, Bose-Bose mixtures, as predicted by D. Petrov, and in one-component BEC systems, as discovered by T. Pfau's group.

In the thesis, we study quantum droplet properties using the so-called Lieb-Liniger Gross-Pitaevskii equation (LLGPE), which allows studying a strongly-interacting one-dimensional Bose system without invoking quantum corrections. That is possible due to the exact solution given by E. Lieb. We build the LLGPE using the hydrodynamical approach and the Lieb-Liniger chemical potential. We additionally add the non-local dipolar interaction to the LLGPE, which enables droplet formation.

In this master's thesis, we study stationary solutions to the LLGPE. We conclude that introducing different additional energies to the quantum droplet ground state results in losing particles and droplet shrinking during real-time evolution. Taking into account our observations, we build a simple, phenomenological model of a quantum droplet and investigate its evaporation under temperature. We conclude that the quantum droplet evaporates slower with the increase of the dipolar coupling constant g_{dd}.

Keywords: quantum droplets, bosons, ultracold atoms, 1D

Własności kropel kwantowych w niezerowej temperaturze

W pracy badany jest jednowymiarowy, silnie oddziałujący gaz bozonów z dodatkowym nielokalnym członem dipolowym. W układach takich mogą powstawać zupełnie nowe formy ultra rozrzedzonej materii – krople kwantowe. Formowanie się kropli kwantowych jest możliwe w ultra zimnnych układach bozonów, w których występują dwa typy oddziaływań o różnej naturze – przyciągającej i odpychającej. Przeciwne oddziaływania powodują, że w średnio-polowym opisie kondensatu Bosego-Einsteina, może dojść do sytuacji kiedy człon średnio-polowy będzie bliski zeru a znaczącą rolę zaczną odgrywać zwykle pomijane poprawki kwantowe. Opisana sytuacja jest możliwa zarówno w mieszaninach bozonów, co zostało przewidziane przez D. Petrov'a, jak i w jednoskładnikowych układach bozonów, co zaobserwowała grupa prowadzona przez T. Pfau.

W pracy zanalizowano własności kropel kwantowych używając równania Lieba-Linigera Grossa-Pitajewskiego (LLGPE), które opisuje jednowymiarowy układ Bosego bez konieczności wprowadzania poprawek kwantowych. Równanie opiera się na ścisłym rozwiązaniu podanym przez E. Lieb'a. Wykorzystując potencjał chemiczny Lieba-Linigera oraz podejście hydrodynamiczne, wyprowadzono LLGPE oraz dodano do niego dodatkowy nielokalny człon oddziaływania dipolowego. Człon ten umożliwia tworzenie się kropli.

W pracy magisterskiej badano rozwiązania stacjonarne LLGPE. Wprowadzanie dodatkowej energii do stanu podstawowego kropel kwantowych powoduje, że podczas ewolucji w czasie rzeczywistym z kropli wypadają cząstki a ona sama ulega skurczeniu. Biorąc pod uwagę obserwacje, zaproponowano prosty fenomenologiczny model kropli kwantowej i zanalizowano jej parowanie pod wpływem temperatury. Modelowana kropla kwantowa paruje wolniej dla większych stałych sprzężenia oddziaływania dipolowego g_{dd}.

Słowa kluczowe: krople kwantowe, bozony, ultrazimne atomy, 1D

załącznik nr 3 do zarządzenia
nr 28 /2016 Rektora PW

Politechnika Warszawska

……..
miejscowość i data

……..
imię i nazwisko studenta

……..
numer albumu

…….…….
kierunek studiów

OŚWIADCZENIE

Świadomy/-a odpowiedzialności karnej za składanie fałszywych zeznań oświadczam, że niniejsza praca dyplomowa została napisana przeze mnie samodzielnie, pod opieką kierującego pracą dyplomową.

Jednocześnie oświadczam, że:

- niniejsza praca dyplomowa nie narusza praw autorskich w rozumieniu ustawy z dnia 4 lutego 1994 roku o prawie autorskim i prawach pokrewnych (Dz.U. z 2006 r. Nr 90, poz. 631 z późn. zm.) oraz dóbr osobistych chronionych prawem cywilnym,
- niniejsza praca dyplomowa nie zawiera danych i informacji, które uzyskałem/-am w sposób niedozwolony,
- niniejsza praca dyplomowa nie była wcześniej podstawą żadnej innej urzędowej procedury związanej z nadawaniem dyplomów lub tytułów zawodowych,
- wszystkie informacje umieszczone w niniejszej pracy, uzyskane ze źródeł pisanych i elektronicznych, zostały udokumentowane w wykazie literatury odpowiednimi odnośnikami,
- znam regulacje prawne Politechniki Warszawskiej w sprawie zarządzania prawami autorskimi i prawami pokrewnymi, prawami własności przemysłowej oraz zasadami komercjalizacji.

Oświadczam, że treść pracy dyplomowej w wersji drukowanej, treść pracy dyplomowej zawartej na nośniku elektronicznym (płycie kompaktowej) oraz treść pracy dyplomowej w module APD systemu USOS są identyczne.

.....
czytelny podpis studenta

Contents

1. Introduction

1.1. Bose-Einstein condensate

Cooling the gas composed of bosons confined in a harmonic trap causes more particles to occupy lower states of the trap. Decreasing a temperature further toward the absolute zero leads to a quantum state, where almost all particles are located in the ground state. This phenomenon is known as the Bose-Einstein condensation (BEC) and was predicted nearly 100 years ago by A. Einstein.

It might seem that under such cold conditions, there should be a phase transition to the solid state due to three-body collisions. These collisions cause the formation of molecules and crystallisation of the system. Nevertheless, it does not happen immediately. If a gas is very diluted, where the interparticle distance is much larger than the interaction range, then the two-body collisions can prevail over three-body ones. The energy conservation forbids creating molecules and crystallising of a system due to two-body interactions only [1]. Thus cold and diluted conditions allow observing quantum mechanical effect on a macroscopic level.

Cooling atomic vapour to temperatures of nano Kelvins (nK) where quantum effects occur, is a challenge. However, this may be achieved with Doppler cooling and evaporative cooling. Doppler cooling is a method involving opposing laser beams with energy lower than the energy difference between levels in an atom [2]. In the case when an atom absorbs a photon, it will be excited to a higher energy state. If the photon comes from the opposite beam, the atom will slow down. Obviously, not all photons come from the opposite direction. The crucial fact is the position of the resonance frequency, which allows to absorb photons from the a relevant beams. That cooling method assures temperatures of around mK [2]. However, it is still too hot, and the second method is necessary. In evaporative cooling, one reduces the depth of the potential trap confining the atoms, permitting high-energy particles to escape therefore cooling the system. In this way, one may reach the temperature of the condensation.

The first observations of the BEC in cold gases took place in 1995 when three various groups studying ultra-cold atoms observed the BEC in systems of rubidium [3], sodium [4], and lithium [5] gases. Six years later, E. Cornell, C. Wieman and W. Ketterle were honoured with the Nobel prize for conducting experiments on BEC and studying its properties. In 1995's experiments, the primary role was played only by short-range interactions. In the case of ultracold and dilute bosons, they are well approximated by a zero-range contact potential $V(\boldsymbol{r}) = g\delta(\boldsymbol{r})$, where g, $\delta(\boldsymbol{r})$ and $\boldsymbol{r}$, denote respectively a coupling constant, Dirac delta and a relative position. Moreover, these interactions may be thoroughly manipulated using Feshbach resonances [6] – nowadays a standard tool, demonstrated for the first time in a BEC of sodium atoms in 1998 [7]. Confirmation of the condensation and the possibility of precise control of the strength of interparticle forces stimulated further

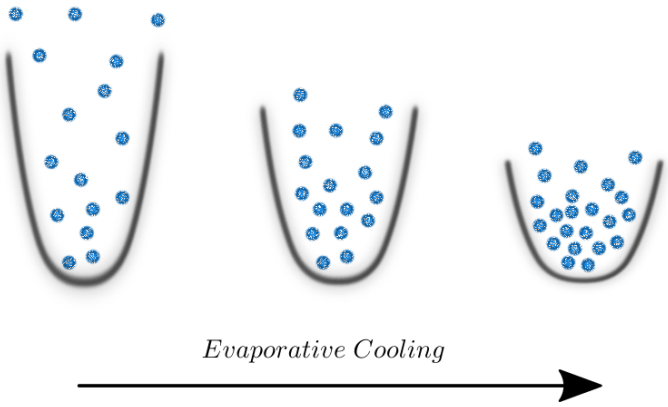

Figure 1.1. Simple visualisation of the evaporative cooling. Decreasing the trap height causes escaping of high-energy particles.

studies and another experiment on BECs. New subjects of investigation became dipolar interactions, i.e. interactions with long-range properties [8, 9]. Studies on condensates consisting of chromium atoms with large magnetic dipole moments proved that around unstable solutions stationary wave functions have new internal structures [8]. Several years later, scientists carried out an experiment on such a system [10], which allowed for a detailed analysis of dipolar quantum gases [11]. However, it turns out that BEC offers a whole new family of exciting phenomena.

1.2. Formation of quantum droplets

The combination of two types of interactions, non-local and short-range, has led to a new state of ultra dilute liquid - a self-bound quantum droplet arising directly from a BEC. A quantum droplet was observed for the first time in 2016 by a group led by T. Pfau [12] and was predicted shortly before by D. Petrov in 2015 in a two-component BEC [13]. At first glance, according to Van der Waals' theory [14], a liquid should not be formed in such a dilute system as a BEC. Nevertheless, this is possible due to quantum fluctuations that contribute a correction to the mean-field description of BEC. The corrections were computed by Lee, Huang and Yang (LHY) in the 1950s [15].

The many-body description of the system is difficult to handle. To predict the basic properties of a many-body system one uses usually approximated methods. The simplest is the mean-field theory, which assumes that particles occupy only one state although interactions may perturb it. According to that, the energy density of a condensed weakly interacting uniform Bose system reads

$$\frac{\varepsilon}{V} = \frac{1}{2} g n^2, \tag{1.1}$$

where n denotes the system's density and V is the system's volume. However, in some physical situations, it turns out that corrections to mean-field energy are relevant. The first

is the LHY correction, which takes into account that BEC undergoes fluctuations even at $T = 0$. The reason for that are interactions between particles, which cause non-condensed states still have a small and fluctuating occupation. Therefore, Eq. (1.1) has an additional term as follows[1]

$$\frac{\varepsilon}{V} = \frac{1}{2} g n^2 + \alpha_{\mathrm{LHY}} (g n)^{5/2}, \tag{1.2}$$

where α_{LHY} is a constant. For a typical one-component BEC system, both terms in Eq. (1.2) have the same sign, and nothing interesting happens. However, a new effect may appear, when these kinds of corrections become dominant. It happens where there are two contributions to the mean-field energy, with different signs, such that the contributions almost cancel each other. Such a situation can take place for instance in a Bose-Bose mixture. Then the energy density (1.1) is modified and reads

$$\frac{\varepsilon_{\mathrm{MIX}}}{V} = \frac{1}{2} g_{11} n_1^2 + \frac{1}{2} g_{22} n_2^2 + g_{12} n_1 n_2, \tag{1.3}$$

where g_{11}, g_{22} are intraspecies coupling constants, meanwhile g_{12} is interspecies one and n_1, n_2 denotes densities of the first and the second component. Such a system may be miscible in the case when effective interactions are repulsive and dominate over inter-component forces and immiscible if interspecies interactions prevail. In the last case, when g_{12} is negative, it may happen in the mean-field theory that the gas collapses, in the process known as Bose-Nova [16]. In the special case, when the mean-field term is close to zero due to the opposite signs of the interactions, the dominant role may be played by the LHY correction. In this situation, the system can form a liquid instead of collapsing [13]. In such a case, the LHY term depends on intra- and interspecies coupling constants and stabilises the droplet against collapse. That is the situation D. Petrov has considered [13]. The experiment with mixtures was carried out in 2018 and confirmed Petrov's predictions [17].

On the other hand, the result obtained by T. Pfau's group [12] was completely unexpected. The primary assumption of this experiment was the investigation of condensate excitation owing to a change in the interactions. The used system was a one-component BEC with dysprosium atoms characterised by huge magnetic moments. The expectation was that the system would shrink due to the impact of the attractive forces and finally explode. Nevertheless, such a situation did not arise, but the system spontaneously formed groups of atoms. These newly created forms were characterised by relatively long lifetime and superfluidity. The responsible for this phenomenon was dysprosium, which is characterised by repulsive interactions and anisotropic long-range dipolar ones that make a liquid stable possible. Shortly afterwards, an analogous experiment was conducted by

[1] Note that it concerns a three-dimensional system. In lower dimensions, the LHY term may have a slightly different form and sign.

F. Ferlaino's group, where quantum droplets were also observed [18]. That group used erbium atoms, which have similar properties to dysprosium ones.

The formation of quantum droplets appears natural, provided that there are interactions of a different nature in the system. The competing forces ensure that one may reach a constant density, thereby obtaining a local energy minimum. Thus, quantum droplets may be created in both Bose-Bose mixtures and one-component BECs with dipolar interactions. Moreover, the last years showed the phenomenon also occurs in lower dimensions [19–21], and additionally, researchers investigated the excitation spectrum of the 1D systems [22, 23].

1.3. Motivation and structure of thesis

In this thesis, we investigate a one-dimensional Bose system with extremely strong effective repulsive forces and non-local weak anisotropic dipolar interactions with attractive nature. It turned out, that in such a system it is also possible to create a quantum droplet [24]. In that paper, the so-called Lieb-Liniger Gross-Pitaevskii equation (LLGPE) was used [25–28]. The LLGPE provides new opportunities to investigate one-dimensional quantum droplets. This is possible by the Lieb-Liniger description, which is the exact description of an interacting one-dimensional Bose system [29, 30]. In this model, the ground state energy of the one-dimensional BEC is known for any strength of the interaction. Therefore, there is no necessity to introduce the LHY correction to the system's description, and the droplet arises from effects beyond the mean-field theory.

So far, the properties of such systems are not well-known. In particular, the thermodynamics of droplets is not fully understood. Therefore, the main goal of the thesis is to investigate its behaviour depending on finite temperature. For this purpose, in Section 2, we discuss theoretical aspects of the LLGPE, starting from the many-body problem and introducing respective interaction terms. Subsequently, in Section 3, we model and present the behaviour of quantum droplets subjected to some perturbation, concluding about various ways and amounts in which energy is added to the system. The last two sections are based on observations and conclusions from the preceding sections, and literature [23, 24]. In these sections, we propose a simplified model of a one-dimensional quantum droplet. For this purpose, in Section 4, we discuss statistical ensembles and the transition of the system's description from grand canonical ensemble to canonical one using Cauchy's integration formula. In order to verify that method, we present well-known results for typical BECs. Finally, in Section 5, we create and analyse a phenomenological model of a one-dimensional quantum droplet and present the numerical results using the method derived in Section 4.

2. Theory of many-body quantum mechanics for bosonic systems

This section introduces the basics of many-body quantum mechanics for bosonic systems. We derive the Hamiltonian of a many-body Bose system in the second quantisation formalism and derive the well-known Gross-Pitaevskii equation (GPE). Next, we focus on the Lieb-Liniger model, for which one finds formulas for eigenenergies for any interaction strength. We use them to construct LLGPE. Finally, we add the anisotropic dipolar term to LLGPE, which makes it possible to study one-dimensional quantum droplets.

2.1. Hamiltonian of many-body Bose system

The quantum-mechanical description of the many-body systems is still challenging. Nevertheless, one may obtain appropriate equations using second quantisation formalism and the mean-field theory. Especially the second theory owes its popularity, among other things, to the approximate description of BECs.

The derivation and the subsequent presentation of the general form of the many-body Hamiltonian and the Gross-Pitaevskii equation primarily relies on the Ref. [1]. Let us consider a one-dimensional system consisting of N ultra-cold interacting bosons. Interaction between particles is described by the two-body interatomic potential $V(x_i - x_j)$. Such a system may be expressed by the following Hamiltonian [1]

$$\hat{H} = \sum_{i=1}^{N} \left[-\frac{\hbar^2}{2m} \frac{\partial^2}{\partial x_i^2} + V_{\mathrm{ex}}(x_i) \right] + \frac{1}{2} \sum_{i \neq j=1}^{N} V(x_i - x_j), \tag{2.1}$$

where $V_{\mathrm{ex}}(x_i)$ is an external trapping potential. We focus on bosons, therefore we look for eigenstates of $\hat{H}$ that are symmetric upon particles exchange. It is beneficial to use here the Fock states. Writing these states in Fock space, one does not care which particle occupies which state but only how many particles are in a specific state. In this case, the wave function may be written as

$$|\psi\rangle = \sum_n c_n |\boldsymbol{n}\rangle, \quad |\boldsymbol{n}\rangle = |n_0, n_1, n_2, ...\rangle. \tag{2.2}$$

where c_n and $|\boldsymbol{n}\rangle$ are respectively expansion coefficients and eigenstates in a Fock basis. We use bosonic creation and annihilation operators $\hat{a}_i^\dagger$ and $\hat{a}_i$, respectively, i.e. the operators obeying

$$\left[\hat{a}_i, \hat{a}_j^\dagger\right] = \delta_{ij}, \quad \hat{a}_i^\dagger |n_i\rangle = \sqrt{n_i + 1}\, |n_i + 1\rangle, \quad \hat{a}_i |n_i\rangle = \sqrt{n_i}\, |n_i - 1\rangle, \quad \hat{a}_i |0\rangle = 0. \tag{2.3}$$

where $|0\rangle$ is the vacuum state (a state without any particle). Furthermore $\hat{a}_i^\dagger \hat{a}_i = \hat{n}_i$ is the particle number operator. Using $\hat{a}_i^\dagger$ one may write any state as follows

$$|n_i\rangle = \frac{1}{\sqrt{n_i!}} \left(\hat{a}_i^\dagger\right)^{n_i} |0\rangle\,, \quad |\boldsymbol{n}\rangle = \prod_{i=0}^{N} \frac{1}{\sqrt{n_i!}} \left(\hat{a}_i^\dagger\right)^{n_i} |0\rangle\,. \tag{2.4}$$

The equation (2.1) can be reformulated with the help of the creation and annihilation operators as follows [1]

$$\hat{H} = \sum_{i=0}^{\infty} \varepsilon_i \hat{a}_i^\dagger \hat{a}_i + \frac{1}{2} \sum_{i,j,i',j'} V_{i,j,i',j'} \hat{a}_i^\dagger \hat{a}_j^\dagger \hat{a}_{i'} \hat{a}_{j'}, \tag{2.5}$$

where ε_i is the energy of the i-th level of the trap which corresponds to a single-particle wave function $\phi_i(x)$

$$\varepsilon_i = \langle i|\, \hat{H}_{\text{non-int}}\, |i\rangle = \int dx\, \phi_i^*(x) \left[-\frac{\hbar^2}{2m}\frac{\partial^2}{\partial x^2} + V_{\text{ex}}(x)\right] \phi_i(x). \tag{2.6}$$

Similarly one can define the matrix elements $V_{i,j,i',j'}$ expressing the interaction terms

$$V_{i,j,i',j'} = \left\langle i, j \middle|\, \hat{V} \,\middle| i', j' \right\rangle = \int dx\, dx'\, \phi_i^*(x) \phi_j^*(x') V(x - x') \phi_{i'}(x) \phi_{j'}(x'). \tag{2.7}$$

Using Eq. (2.5) one may investigate the ground state and other physical properties of the system.

2.2. Gross-Pitaevskii equation for weakly effective interactions

Solving the exact many-body Schrödinger equation is a difficult problem One of the most widely-used methods is the mean-field approach, which allows for studying trapped weakly interacting bosons efficiently [31]. Suppose that in temperature $T = 0$ all bosons occupy the same lowest energy state of a trap. Such a situation corresponds to a well-known phenomenon, i.e. the Bose-Einstein condensation. A wave function of the ideal (without interactions) Bose system may be expressed as a product when all particles are in the same single-particle quantum state

$$\psi_{\text{BEC}}(x) = \phi(x_1)\, \phi(x_2) \ldots \phi(x_N) = \prod_{i=1}^{N} \phi(x_i). \tag{2.8}$$

Once interactions between particles are accounted for, such a wave function constitutes only some approximation. To derive an approximate equation which describes condensate, one might use the Heisenberg equation with many-body Hamiltonian (2.5) and boson field operator or apply a variational procedure. However, before we do that, let us make

some assumptions about $V(x-x')$. For a dilute[2] and cold gas the interaction potential $V(x-x')$ may be replaced by an effective interaction, characterised by a single parameter (scattering length a) [31]

$$V(x-x') = g\delta(x-x'), \quad g = \frac{4\pi\hbar^2 a}{m}, \tag{2.9}$$

where g is the coupling constant. Interactions are repulsive if $g > 0$ and attractive when $g < 0$. This potential was initially introduced by E. Fermi and has the same properties at a low-energy regime as the exact potential [32]. Now we compute the average value of the energy operator, given in Eq. (2.5) in the state $\psi_{\mathrm{BEC}}(x)$. The direct computations give

$$E[\phi,\phi^*] = N\int dx\left[-\frac{\hbar^2}{2m}\phi^*(x)\frac{\partial^2}{\partial x^2}\phi(x) + V_{\mathrm{ex}}(x)\left|\phi(x)\right|^2 + \frac{g}{2}(N-1)\left|\phi(x)\right|^4\right]. \tag{2.10}$$

The expression above denotes the energy functional with normalisation $\int dx\left|\phi(x)\right|^2 = 1$. Introduce Lagrange multiplier μ causes that minimalisation condition takes the following form

$$\mu\,\phi(x) = \left[-\frac{\hbar^2}{2m}\frac{\partial^2}{\partial x^2} + V_{\mathrm{ex}}(x) + gN\left|\phi(x)\right|^2\right]\phi(x), \tag{2.11}$$

where the Lagrange multiplier μ corresponds to a chemical potential of the system. On the mean-field level, we may neglect "-1" in the $(N-1)$ expression, which we have done above. Equation (2.11) is the stationary Gross-Pitaevskii equation. It has also a time-dependent version

$$i\hbar\frac{\partial}{\partial t}\phi(x,t) = \left[-\frac{\hbar^2}{2m}\frac{\partial^2}{\partial x^2} + V_{\mathrm{ex}}(x) + gN\left|\phi(x,t)\right|^2\right]\phi(x,t). \tag{2.12}$$

The validity of GPE assumes that scattering length a is much smaller than the average interatomic distance [31]. It has been proved that GPE correctly describes weakly interacting bosons, including low-energy excitations and solitons [33]. Nevertheless, it turns out that even in this regime, the equation may not predict interesting phenomena such as quantum depletion [34, 35].

2.3. Exact description of the interacting Bose gas - Lieb-Liniger model

In the previous subsection, we discussed the GPE for weak effective interactions, where the condensed Bose system may be described using the mean-field approximation with a single-particle non-linear Schrödinger equation. Nevertheless, such an equation does not take into account mutual quantum correlations and LHY correction. One solution to studying quantum droplets is adding that correction, which is relatively simple for three-dimensional systems. In that way, one can adequately describe Bose-Bose mixtures and dipolar quantum gases. The situation becomes more challenging when one

[2] Saying "dilute" we mean that $na^3 \ll 1$ condition is met, where n and a denotes respectively gas density and scattering length.

wants to investigate lower dimensions or arbitrarily strong interactions, where quantum fluctuations are significantly enhanced. In such a regime, LHY is not applicable.

On the other hand, in 1D there is a known exact solution to a quantum many-body model of interacting bosons, even in the case of strong interparticle correlations. This model, known as the Lieb-Liniger (LL) model [29, 30], assumes interaction potential in the form $V(x-x') = g\delta(x-x')$, which allows to study homogeneous gas with short-range forces, i.e. the topic of this master's thesis. The ground state energy, found in [29], reads

$$\varepsilon_0(N,L) = \frac{\hbar^2}{2m}\frac{N^3}{L^2}e_{\mathrm{LL}}(\gamma), \quad \gamma = \frac{m}{\hbar^2}\frac{gL}{N}, \tag{2.13}$$

where γ is the dimensionless Lieb parameter and $e_{\mathrm{LL}}(\gamma)$ is a monotonically increasing function of γ. That function does not have an explicit form, but in the limit of $N, L \to \infty$ with $\rho = N/L = \text{const}$ can be found with the Fredholm integral equations [30]. Nevertheless, it is known with extremely accurate approximation as polynomial [36] (see appendix A). There are three general regimes for $e_{\mathrm{LL}}(\gamma)$. In the case when $\gamma = 0$, there are no effective interactions and $e_{\mathrm{LL}}(\gamma) = 0$. For weakly interacting particles i.e. $\gamma \ll 1$, one has $e_{\mathrm{LL}}(\gamma) \approx \gamma - 4\gamma^{3/2}/(3\pi)$, where the negative term may be taken as the LHY correction. For infinitely strong forces i.e. $\gamma \to \infty$, we have $e_{\mathrm{LL}}(\gamma) \approx \pi^2/3$, which gives Girardeau's ground state solution of extremely strong repulsive bosons [37]. Now, with the ground state energy (2.13), we may calculate pressure $p_{\mathrm{LL}}(N,L)$ and chemical potential $\mu_{\mathrm{LL}}(N,L)$ as appropriate derivatives [23, 38]

$$p_{\mathrm{LL}}(N,L) = -\frac{\partial}{\partial L}\varepsilon_0(N,L) = \frac{\hbar^2}{2m}\frac{N^3}{L^3}\left[2e_{\mathrm{LL}}(\gamma) - \gamma\frac{\partial}{\partial\gamma}e_{\mathrm{LL}}(\gamma)\right] \tag{2.14}$$

$$\mu_{\mathrm{LL}}(N,L) = \frac{\partial}{\partial N}\varepsilon_0(N,L) = \frac{\hbar^2}{2m}\frac{N^2}{L^2}\left[3e_{\mathrm{LL}}(\gamma) - \gamma\frac{\partial}{\partial\gamma}e_{\mathrm{LL}}(\gamma)\right]. \tag{2.15}$$

We aim to derive an equation that properly describes interacting Bose gas with any strength of short-range forces. We may introduce an adequate equation via quantum hydrodynamics equations using an exact solution to the ground state energy and thereby the pressure and chemical potential. That is a more general approach and alternative formulation of the Schrödinger equation introduced by E. Madelung. Assuming we treat an atomic cloud as divided into small parts, but at the same time, these consist of many particles, one may write Euler and continuity equations as follows

$$\frac{\partial}{\partial t}\rho + \frac{\partial}{\partial x}(\rho v) = 0, \tag{2.16}$$

$$\frac{\partial}{\partial t}v + v\frac{\partial}{\partial x}v = -\frac{1}{m\rho}\frac{\partial}{\partial x}p, \tag{2.17}$$

where $\rho \equiv \rho(x,t)$, $v \equiv v(x,t)$ and $p \equiv p(x,t)$ denotes respectively local gas density, velocity

of particles cloud and pressure. What is more, we assume local equilibrium in each of these parts under [39]. The equation (2.17) may also consist of so-called quantum pressure, which may be neglected considering slow-changing density [26]. Now by comparing (2.14) and (2.15) we may write the Euler equation as[3]

$$\frac{\partial}{\partial t}v + v\frac{\partial}{\partial x}v = -\frac{1}{m}\frac{\partial}{\partial x}\mu_{\mathrm{LL}}\left[\rho\right]. \tag{2.18}$$

Introducing one complex field

$$\phi(x,t) = \sqrt{\frac{\rho(x,t)}{N}}e^{i\varphi(x,t)} \quad \text{with} \quad \frac{\hbar}{m}\frac{\partial}{\partial x}\varphi(x,t) = v(x,t), \tag{2.19}$$

we combine continuity and Euler equations into [25, 26] (see appendix B for evidence)

$$i\hbar\frac{\partial}{\partial t}\phi(x,t) = \left[-\frac{\hbar^2}{2m}\frac{\partial^2}{\partial x^2} + \mu_{LL}\left[N|\phi|^2\right]\right]\phi(x,t), \tag{2.20}$$

where

$$\mu_{LL}\left[N|\phi|^2\right] = \frac{\hbar^2}{2m}N^2|\phi|^4\left[3e_{\mathrm{LL}}\left(\frac{\kappa}{N|\phi|^2}\right) - \frac{\kappa}{N|\phi|^2}e'_{\mathrm{LL}}\left(\frac{\kappa}{N|\phi|^2}\right)\right], \quad \kappa = \frac{gm}{\hbar^2}. \tag{2.21}$$

The expression (2.20) is the Lieb-Liniger Gross-Pitaevskii equation and was used, among other things, for a description of shock waves [26, 27]. Let us consider two regimes of LLGPE. For weakly interacting particles the function $e_{\mathrm{LL}}(\gamma)$ in the first approximation order is $e_{\mathrm{LL}}(\gamma) \approx \gamma$ and $\mu_{LL}\left[N|\phi|^2\right] = gN|\phi|^2$. We see that we obtained the mean-field term from the Gross-Pitaevskii equation. The second regime are extremely repulsive contact interactions with $e_{\mathrm{LL}}(\gamma) \approx \pi^2/3$ and we obtain the equation proposed by Kolomeisky [40]

$$i\hbar\frac{\partial}{\partial t}\phi(x,t) = \left[-\frac{\hbar^2}{2m}\frac{\partial^2}{\partial x^2} + \frac{\hbar^2\pi^2}{2m}N^2|\phi|^4\right]\phi(x,t). \tag{2.22}$$

At first, it seems pointless to introduce an effective mean-field-like model like as (2.20), for a many-body system which is exactly solvable, i.e. the LL model. On the other hand, the many-body solutions of E. Lieb are not handy, and still, they are often studied numerically with results limited to a small number of atoms only. The equation (2.20) is, therefore, helpful to study large systems still giving reliable results for strong interactions (see benchmarks in [41]). Moreover, Eq. (2.20) is a good starting point to construct models extending the LL description, where for instance, also other types of interaction potentials are present.

[3] Notice that we assumed a slow-changing density profile which allows us to significantly simplify comparing pressure with chemical potential because of appropriate derivative over density towards zero.

2.4. Extension of Lieb-Liniger model to dipolar interactions

So far, we have restricted the description of a system to short-range forces only. On the other hand, a quantum droplet may emerge due to the interplay between the short- and long-range dipolar interactions. Generally, magnetic dipole interaction between two particles with dipole moments $\boldsymbol{\mu_1}$, $\boldsymbol{\mu_2}$ and positions $\boldsymbol{r_1}$, $\boldsymbol{r_2}$ has the following form [42]

$$V_{\mathrm{dd}}\left(\boldsymbol{r_1},\boldsymbol{r_2}\right)=\frac{\mu_0}{4\pi}\left[\frac{\boldsymbol{\mu_1}\cdot\boldsymbol{\mu_2}}{r^3}-\frac{3\left(\boldsymbol{\mu_1}\cdot\boldsymbol{r}\right)\left(\boldsymbol{\mu_2}\cdot\boldsymbol{r}\right)}{r^5}\right], \tag{2.23}$$

where μ_0 is the vacuum permeability and $r=\left|\boldsymbol{r}\right|=\left|\boldsymbol{r_1}-\boldsymbol{r_2}\right|$. Supposing we consider one kind of dipolar gas polarised along one direction we may write that

$$V_{\mathrm{dd}}\left(\boldsymbol{r_1},\boldsymbol{r_2}\right)=\frac{\mu_0\mu_D^2}{4\pi}\frac{1-3\cos^2\left(\theta\right)}{r^3},\quad \cos\left(\theta\right)=\frac{\boldsymbol{\mu_D}\cdot\boldsymbol{r}}{\left|\boldsymbol{\mu_D}\right|\cdot\left|\boldsymbol{r}\right|},\quad \boldsymbol{\mu_D}\equiv\boldsymbol{\mu_1}=\boldsymbol{\mu_2}. \tag{2.24}$$

Properties of dipolar interactions are related to dipole placement, thus these are anisotropic interactions. In general, one may distinguish between two cases, i.e. repulsive and attractive dipolar interactions. In the case when dipoles are configured in head-to-tail ($\rightarrow\rightarrow$) position, then $1-3\cos^2\left(0\right)<0$ and forces are attractive. For side-by-side ($\uparrow\uparrow$) configurations these are repulsive, i.e. $1-3\cos^2\left(\pi/2\right)>0$. Now we want to extend that dipolar

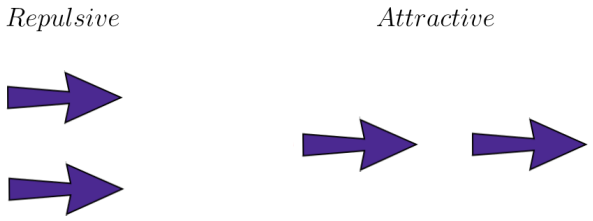

Figure 2.1. Sketch of specific dipole configurations. Side-by-side configuration causes repulsive interactions. Head-to-tail configuration causes attractive interactions.

potential to the case of a quasi-one-dimensional harmonic trap, where dipoles are confined in a cigar-shaped harmonic trap [43]. However, before we do that let us make some assumptions about dipolar interaction. In the case of 3D dipole-dipole interaction, it is actually long-range and changes like $1/r^3$. However, if we want to obtain a model of 1D dipolar interaction, one needs to consider the 3D case and assume that atoms are tightly confined in the perpendicular directions (Y and Z) due to a harmonic trap, but free in the X direction. That comes down to the assumption that in every 3D equation, the many-body wave function in perpendicular directions is the Gaussian function. Therefore, further integration results in effective dipolar interaction, which may be written as follows (see [43] for details)

$$V_{\mathrm{dd}}\left(x-x'\right)=-g_{\mathrm{dd}}V_{\mathrm{dd}}^{\sigma}\left(x-x'\right)=-g_{\mathrm{dd}}\frac{1}{\sigma}\widetilde{V}_{\mathrm{dd}}\left(\frac{x-x'}{\sigma}\right), \tag{2.25}$$

with

$$g_{\mathrm{dd}} = -\frac{\mu_0 \mu_D^2}{4\pi} \frac{1-3\cos^2\theta}{\sigma^2}, \tag{2.26}$$

and

$$\widetilde{V}_{\mathrm{dd}}(u) = \frac{1}{4}\left[-2|u| + \sqrt{2\pi}\left(1+u^2\right)\exp\left(\frac{u^2}{2}\right)\mathrm{erfc}\left(\frac{|u|}{\sqrt{2}}\right)\right], \tag{2.27}$$

where erfc is the complementary error function, and $\sigma = \sqrt{\hbar/(m\omega_\perp)}$ denotes the transverse harmonic oscillator length, meanwhile $\omega_\perp$ is the frequency of the trap in perpendicular direction [43]. We consider a head-to-tail ($\rightarrow\rightarrow$) configuration only, therefore throughout the whole thesis we use $g_{\mathrm{dd}} = \mu_0\mu_D^2/\left(2\pi\sigma^2\right)$. We add dipolar interaction exactly in the same way contact interactions are usually included to get the GPE. Therefore, we get the LLGPE extended by dipolar interaction term [8, 9, 11] for specific dipolar potential

$$\begin{aligned} i\hbar\frac{\partial}{\partial t}\phi(x,t) = &\left[-\frac{\hbar^2}{2m}\frac{\partial^2}{\partial x^2} + \mu_{LL}\left[N|\phi|^2\right]\right]\phi(x,t) \\ &- g_{\mathrm{dd}} N\int dx'\, V_{\mathrm{dd}}^{\sigma}(x-x')|\phi(x',t)|^2\phi(x,t). \end{aligned} \tag{2.28}$$

In the special case when $\phi(x,t)$ is in the following form

$$\phi(x,t) = \phi(x)\exp\left(-\frac{i\mu}{\hbar}t\right), \tag{2.29}$$

Eq. (2.28) has the stationary form as follows

$$\mu\,\phi(x) = \left[-\frac{\hbar^2}{2m}\frac{\partial^2}{\partial x^2} + \mu_{LL}\left[N|\phi|^2\right]\right]\phi(x) - g_{\mathrm{dd}} N\int dx'\, V_{\mathrm{dd}}^{\sigma}(x-x')|\phi(x')|^2\phi(x). \tag{2.30}$$

In the subsequent chapter, we will discuss the stationary Lieb-Liniger Gross-Pitaevskii equation with dipolar interaction (2.30). Such an equation offers several types of solutions, i.e. bright solitons, quantum droplets and the special case of quantum droplets, i.e. fermionised quantum droplets, for which an analytical solution is known [23].

3. Numerical results and observations for LLGPE

This chapter presents numerical results of imaginary-time evolution (ITE) and real-time evolution (RTE) methods for the LLGPE. We precisely find the ground state of the quantum droplet using the ITE method. Afterwards, we add energy to that state through some perturbation in the form of noise and observe its evolution in real time. The droplets' behaviour allows us to motivate a model for a droplet at a finite temperature introduced in the following sections.

3.1. Imaginary time evolution

There are several methods to compute the system eigenvalues and eigenstates. One of these is the so-called imaginary time evolution (ITE), e.g. [44]. The method is based on changing the time variable in the propagator for an imaginary time. Therefore, instead of quantum state oscillation, one has the exponential decay of it. Suppose some system is described by wave function $\psi(x)$. The system's state may always be written in the eigenstates base i.e.

$$\big|\psi(x)\big\rangle = \sum_n c_n \big|\psi_n(x)\big\rangle, \tag{3.1}$$

where c_n are expansion coefficients in this base. Time evolution in quantum mechanics is described by the Schrödinger equation

$$i\hbar\frac{\partial}{\partial t}\psi(x,t) = \hat{H}\psi(x,t), \tag{3.2}$$

with the time-independent Hamiltonian $\hat{H}$. In order to find the time dependence of $\psi(x,t)$, we have to solve the eigenvalue equation for the $\hat{H}$

$$\hat{H}\big|\psi_n(x)\big\rangle = E_n\big|\psi_n(x)\big\rangle, \tag{3.3}$$

where $\big|\psi_n(x)\big\rangle$ is the eigenstate and E_n is the eigenvalue of the $\hat{H}$. At any later time, the wave function $\psi(x,t)$ reads

$$\big|\psi(x,t)\big\rangle = \sum_n c_n \exp\left(-\frac{iE_n}{\hbar}t\right)\big|\psi_n(x)\big\rangle. \tag{3.4}$$

This means that each eigenstate oscillates with a frequency proportional to $E_n/\hbar$. When we consider the change of variables $it \to \tau$, we may treat time as an imaginary time. In consequence, we have

$$\big|\psi(x,\tau)\big\rangle = \sum_n c_n \exp\left(-\frac{E_n}{\hbar}\tau\right)\big|\psi_n(x)\big\rangle. \tag{3.5}$$

Here in the imaginary time, we do not have wave function as the oscillating superposition of energy eigenstates but as the exponential decay of these states. For an appropriately long time τ (suppose $\tau \to \infty$, just to indicate that it is a relatively long time), we obtain that

$$\left|\psi(x,\tau\to\infty)\right\rangle \approx c_0 \exp\left(-\frac{E_0}{\hbar}\tau\right)\left|\psi_0(x)\right\rangle, \tag{3.6}$$

where E_0 and $\psi_0(x)$ are respectively the ground state energy and ground state wave function. Given that the E_0 is the lowest energy, the exponential decay in Eq. (3.6) is the slowest. This way, we may obtain the ground state of $\hat{H}$. This method works well in case when some contribution of the ground state exists. Otherwise, one gets just the lowest energy state. Moreover, one has to normalise the wave function in each time step. Otherwise, such an equation will converge to zero.

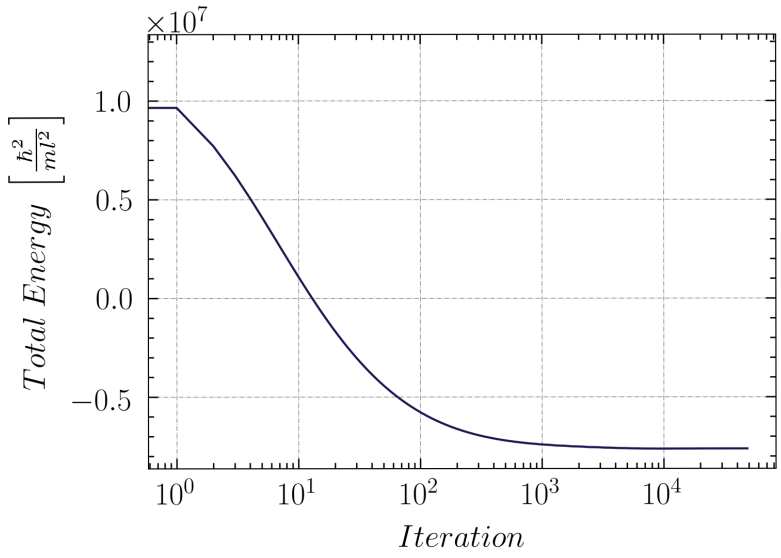

Figure 3.1. Energy convergence to the droplet ground state using the ITE method. The presented case corresponds to the LLGPE following parameters $N = 200$, $g = 20000$, $g_{\mathrm{dd}} = 1000$ and $\sigma = 0.015$.

In what follows, we will use l, $ml^2/\hbar$, $\hbar^2/ml^2$, and $\hbar^2/ml^2k_B$ as the units of length, time, energy, and temperature, respectively.

3.2. Ground states of Lieb-Liniger Gross-Pitaevskii equation

A one-dimensional quantum droplet is one of the peculiar stationary solutions to the LLGPE. There is a regime, hereafter called the analytical regime, in which many properties of stationary solutions can be derived analytically. This regime corresponds to the case when one considers a system with weak long-range dipolar interactions where $\sigma \to 0$ and powerful short-range contact repulsion with $g \to \infty$. Such assumptions substantially simplify the stationary form of LLGPE (2.30). The condition $\sigma \to 0$ causes that dipolar

potential takes the form of a simple delta function, meanwhile the condition $g \to \infty$ allows to replace Lieb-Liniger potential with a constant expression because of $e_{\mathrm{LL}}(\gamma \to \infty) \to \pi^2/3$. One may read more precisely about these assumptions and the limits of their applicability in [23]. Nevertheless, one should wonder about condition $\sigma \to 0$, given that this is a range of non-local effective dipolar potential. In the hydrodynamical approach, it was assumed that σ is much larger than the interparticle distance d. In fact, there are regimes, of $N \to \infty$, in which both d and σ converges to 0, always satisfying the condition $\sigma \gg d$. All of this makes it possible to write the stationary LLGPE as follows

$$\mu\,\phi(x) = \left[-\frac{\hbar^2}{2m}\frac{\partial^2}{\partial x^2} + \frac{\hbar^2\pi^2}{2m}N^2\left|\phi(x)\right|^4 - g_{\mathrm{dd}}N\left|\phi(x)\right|^2\right]\phi(x) \tag{3.7}$$

In this case, solutions are characterised only by two parameters. These are the number of particles N and dipolar coupling constant g_{dd}. Below we present several cases of stationary solutions of quantum droplets in the assumed regime. In Fig. 3.2, we can observe that the

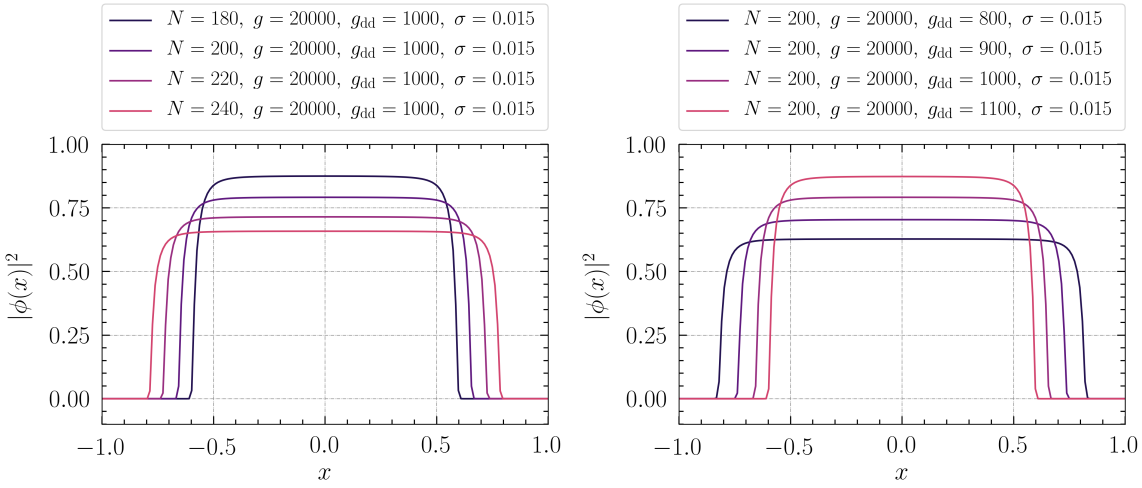

Figure 3.2. Stationary solutions to the LLGPE for different particle numbers (left) and different dipolar coupling constant (right). They present density profiles of one-dimensional quantum droplets obtained using the ITE method.

system's density profile has a flat area where density is with reasonable approximation constant and characteristic edges where it quickly falls. However, before we pay special attention to the adopted parameters, let us introduce a valuable analytical formula. It turns out that the quantum droplet width depends linearly on the number of particles and is inversely proportional to the dipolar coupling constant. That width was found analytically and reads [23]

$$W = \frac{2\pi^2\hbar^2}{3m}\frac{N_{\mathrm{d}}}{g_{\mathrm{dd}}}, \tag{3.8}$$

where $N_{\mathrm{d}} = N$ is the number of particles that compose quantum droplet. Formula (3.8) is valid in the analytical regime introduced above, so only two parameters characterise it. In both cases presented in Fig. 3.2, the effective coupling constant is around 20 times greater

than the dipolar one, which allows us to think that the parameters fulfil the assumptions of the analytical regime. Subsequently, it is worth mentioning the non-local interaction range. Interparticle distance are just a ratio of droplet width W and the number of particles that form it, so $d = W/N$, where W is defined as (3.8). In the left panel of Fig. 3.2, with a different number of particles, that expression is constant and approximately equal to $d \approx 0.0066\, l$. That denotes the dipolar interaction range is around 2.27 times greater than the interparticle distance. In the right panel of Fig. 3.2, with different g_{dd} and the same N one gets values from 1.83 to 2.54. Moreover, the relative errors of numerical widths obtained from the ITE method and analytical formula remain lower than 1%. It is also worth noting that density profiles are similar to rectangular shapes, which will prove crucial when introducing the droplet model in Section 5.

The presence of droplets is not limited to the above-mentioned parameter regime. Below, we present other stationary solutions still droplet-like, but outside that regime. These droplets do not fulfil the analytical width formula (3.8).

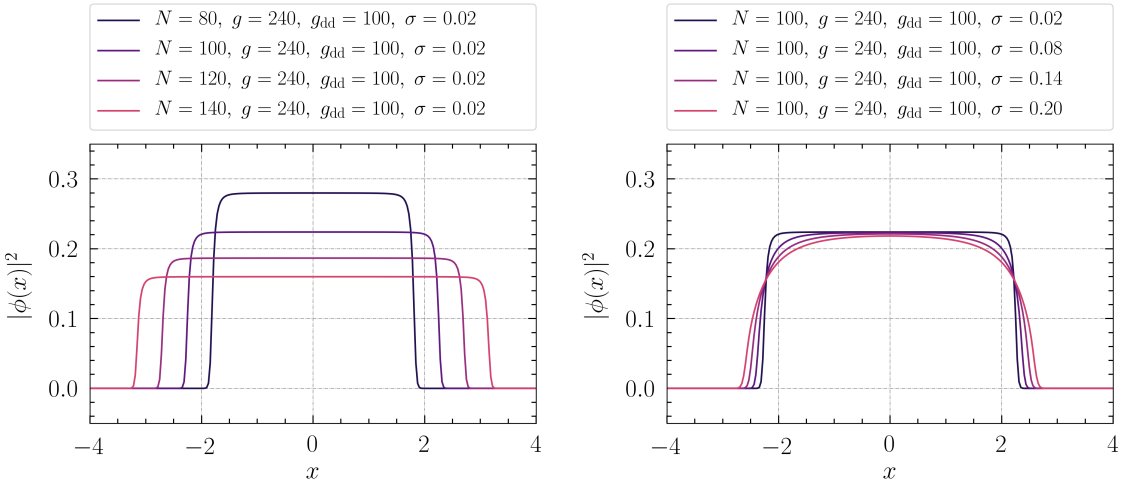

Figure 3.3. Stationary solutions to the LLGPE for different particle numbers (left) and different dipolar interaction range (right). In this case, the analytical regime of LLGPE is not fulfilled.

It turns out that the search for stationary solutions for the strict quantum droplet regime is a difficult numerical task. Even if one finds with the ITE method a candidate for the ground state, one needs to verify it. We use the real-time evolution of such a state and assess whether the density is approximately constant. Failure to meet this condition manifests as "quantum droplet breathing". Of course, for such cases, we were improving our numerics using the ITE method increasing the precision of the calculations.

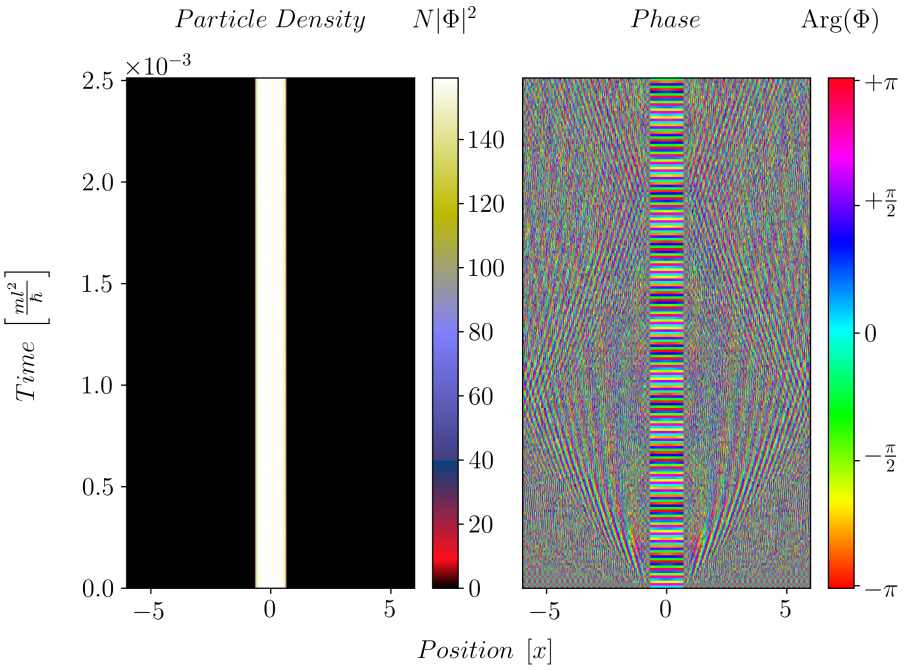

Figure 3.4. Numerical test: Evolution of the solution to the LLGPE in the quantum droplet regime of interactions found with the ITE. The quantum droplet has the following parameters $N = 200$, $g = 20000$, $g_{\text{dd}} = 1000$ and $\sigma = 0.015$.

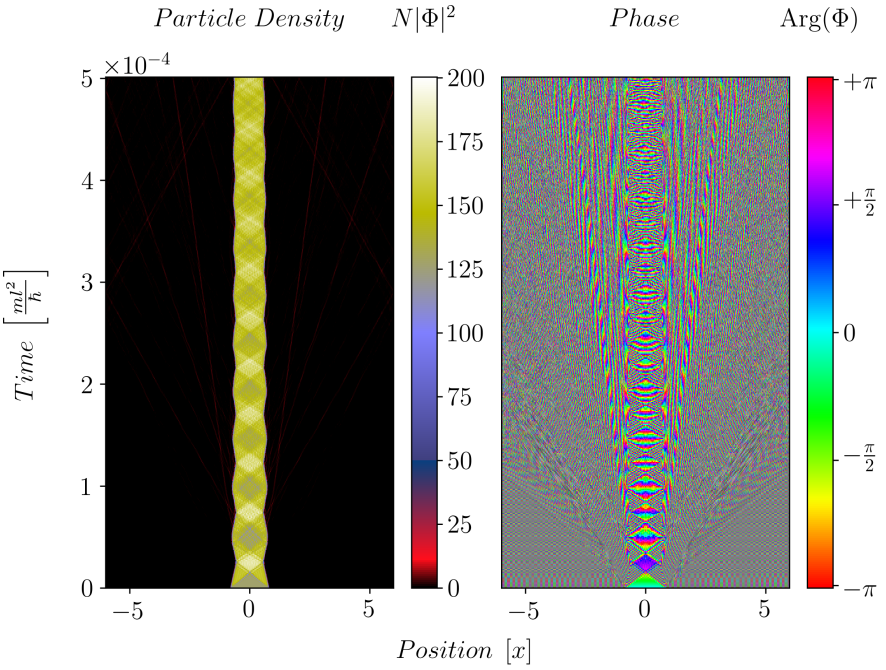

Figure 3.5. The stationary solution, which has been found with too low accuracy. It is characterised by "droplet breathing", which one may observe on the left side of the figure. The system has the same physical parameters as in Fig. 3.4.

3.3. Evolution of perturbed quantum droplets in real time

Conducting the real-time evolution of the ground state, obviously from the definition, cannot change this state. Regardless, in the case when the stationary solution would be in a certain way perturbed, then it is no longer a ground state, and real-time dynamics may be quite complex. It turns out that adding some energy to the system in the ground state may result in emitting particles from a quantum droplet. This is exactly the situation we observed during the simulation. When we introduce some energy to the system, then some particles leave a droplet, and it shrinks according to the formula (3.8). We can therefore expect that adding different energy values to the system will result in different numbers of particles leaving a droplet. For this purpose, we would have to run many simulations for different energies to observe subsequent dynamics. In Fig. 3.6 we show a perturbed

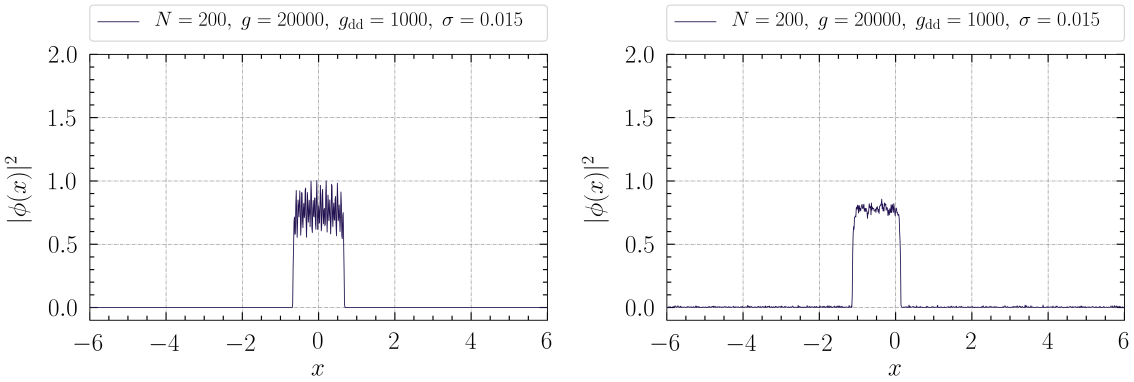

Figure 3.6. The stationary solution to the LLGPE in the analytical interaction regime, perturbed by a noise in the form of a deterministic sine combination. The figure on the left corresponds to a situation before a real-time evolution but with additional energy. The figure on the right presents the system after its evolution.

stationary solution to the LLGPE. In this case, the perturbation is fully deterministic and it is in the form of a linear combination of the sine functions with different but constant weights as follows

$$\xi(x) = A\left[a_1 \sin\left(a_2 f x\right) + b_1 \sin\left(b_2 e f x\right) + c_1 \sin\left(c_2 \pi f x\right)\right], \tag{3.9}$$

where A, a_1, a_2, b_1, b_2, c_1 and c_2 are constants, and f denotes a noise frequency. By adding around 4.5% of ground state energy, we have caused that several particles escaped from the droplet. We perturbed the droplet with different noise functions, including sine function, linear sine combination and random values from uniform and gaussian distributions. For a given added energy, each type of perturbation leads to similar dynamics. We may therefore claim that this phenomenon only depends on the amount of the extra energy but not on the perturbation details.

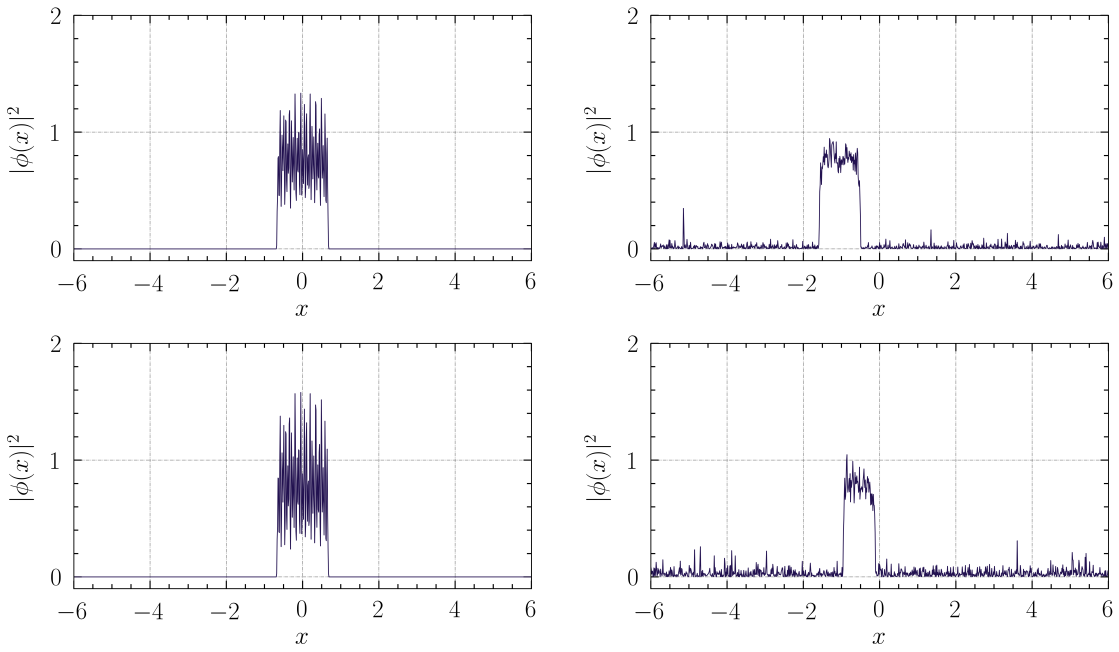

Figure 3.7. Parturbation of stationary solutions to the LLGPE. The system has the following parameters $N = 200$, $g = 20000$, $g_{dd} = 1000$ and $\sigma = 0.015$. Each subsequent row presents the quantum droplet ground state with a certain perturbation. We subsequently introduced 23.5% and 46.1% of ground state energy to the system.

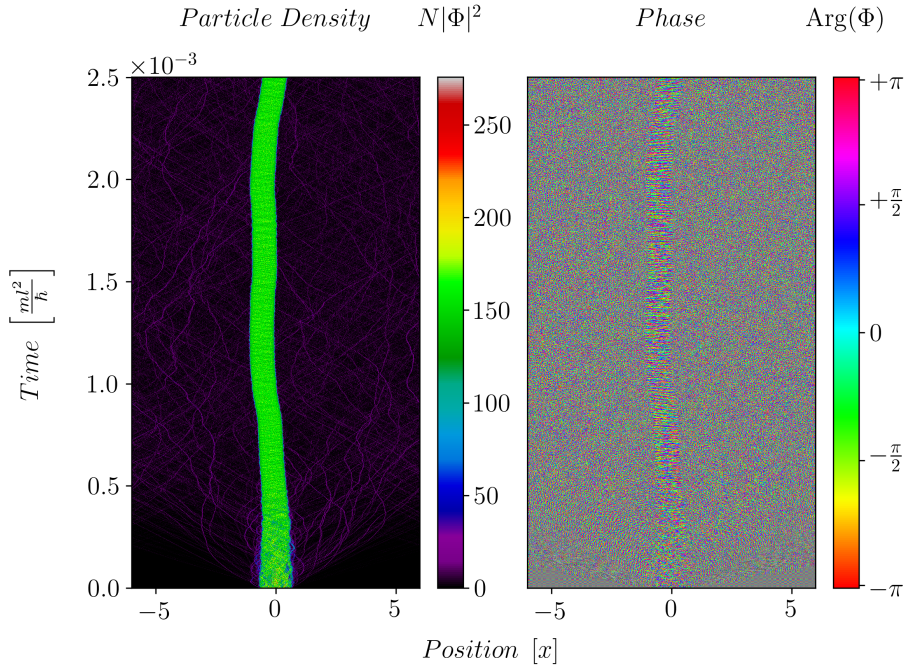

Figure 3.8. Real-time evolution of a disturbed quantum droplet with following parameters $N = 200$, $g = 20000$, $g_{dd} = 1000$ and $\sigma = 0.015$. This is the case in which we added to the system 23.5% of its ground state energy.

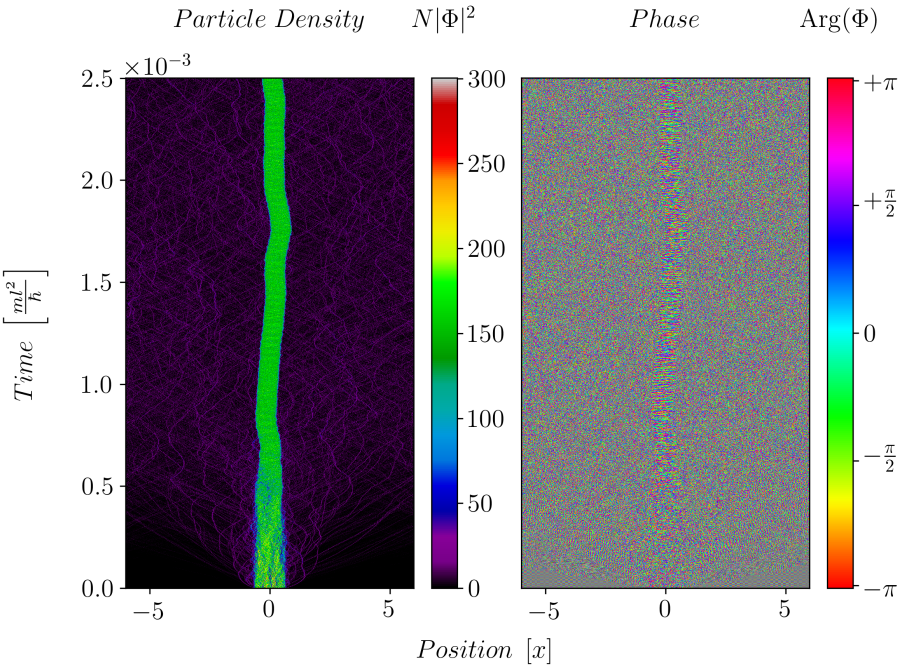

Figure 3.9. Real-time evolution of a disturbed quantum droplet with following parameters $N = 200$, $g = 20000$, $g_{\mathrm{dd}} = 1000$ and $\sigma = 0.015$. In this case, we added 46.1% of the ground state energy. We can easily see that particles leave the droplet.

One may calculate the width of the quantum droplet during evolution. However, this is not a simple problem because the system's dynamic is complicated in the early stages of evolution. Nevertheless, we can do it because we are interested in what is at the end of the evolution, and the dynamic is stabilised there. Thus, we discard the early dynamic and average the droplet width only there, where the dynamic is stabilised. Below we present the figure where one can see perturbed quantum droplet width during evolutions. In Fig.

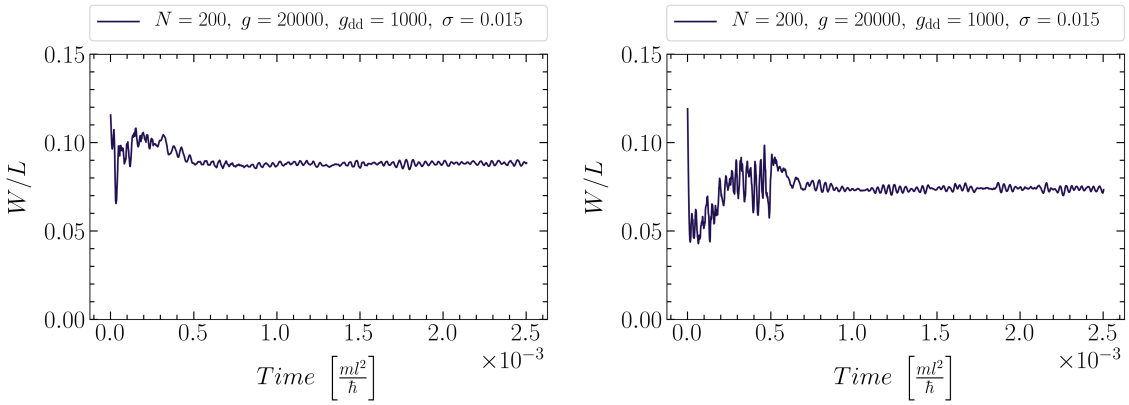

Figure 3.10. Quantum droplet width during real-time evolution. Figures corresponding respectively to 23.5% and 46.1% of ground state energy introduced.

3.10 we may see that the system relatively quickly reaches an equilibrium state. In this way, by adding 23.5% of the ground state energy, the width is reduced from $W/L \approx 0.110$

to $W/L \approx 0.089$, which constitutes a shrinkage of the droplet by around 19%. In turn, introducing 46.1% of the ground state energy reduced this value to $W/L \approx 0.074$, meaning that the system shrinks approximately by 33%. The L parameter denotes the total width of the system and in the above simulations was equal to $L = 12\ l$.

The observations contained in this chapter are as follows. We can see that bringing the system to the ground state is quite challenging because one has to provide high calculation accuracy and fulfil the analytical regime simultaneously. Nevertheless, we can do this for several cases, allowing for a real-time evolution with additional energy from perturbation. It turns out that the introduction of additional energy causes particles to begin leaving the droplet. This phenomenon manifests as droplet shrinkage. With increasing the additional energy value, more particles escape from the droplet, and early evolution is highly complex and difficult to analyse. Moreover, adding a huge amount of energy (of the order of 100% of the ground state energy) causes droplet splits, and only free particles exist in the system. We would like to study how a droplet evaporates due to heating, given that it reaches an equilibrium with the emitted particles. Our observations summarised above motivate us to propose a simplified phenomenological model, which would capture the essential properties of a droplet and allow us to study its statistical properties. Before introducing our model, we will recall the standard methods of statistical mechanics, which will be used in further chapters. Therefore, the following chapters are dedicated to introducing statistical ensembles that are applied to bosonic systems. The last chapter contains the presentation of the simple quantum droplet model.

4. Theory of statistical ensembles for bosonic systems

This chapter introduces necessary properties of statistical ensembles for non-interacting bosons. We use Cauchy's integral formula to compute some properties of the system in the canonical ensemble using the grand canonical one. This procedure gives excellent results for typical BECs.

4.1. Grand canonical ensemble for ideal Bose gas

Statistical physics describes microscopic properties of physical systems consisting of many particles using probability theory. In general, one can distinguish three statistical ensembles. The microcanonical ensemble corresponds to an isolated system with fixed energy E and a fixed number of particles N. It is assumed that each micro-state is equally probable. The second ensemble is the canonical ensemble, with a fixed temperature and number of particles corresponding to a closed system. Such a system may exchange energy with its environment, and the probability of some microscopic state depends on its energy. The last ensemble is the grand canonical ensemble that may exchange energy and particles with its environment, but temperature and chemical potential are fixed. In this case, the probability of a state depends on the energy and the number of particles.

Let us consider an ideal Bose gas. Assuming that a system consists of non-interacting particles, the system might be built up from single-particle states [45]. We may present the total energy and total particle number as follows

$$E = \sum_{i=0}^{\infty} n_i \varepsilon_i, \quad N = \sum_{i=0}^{\infty} n_i. \tag{4.1}$$

where the summation proceeds over all possible available energy states ε_i and the number of the single-particle states n_i. We consider Bose gas, therefore n_i can be 1, 2, 3, ..., ∞. The partition function in the grand canonical ensemble reads

$$\Xi(\mu,\beta) = \sum_{\{n_1,n_2,\ldots\}} \exp\left[-\beta\left(E-\mu N\right)\right], \quad \beta = \frac{1}{k_B T}. \tag{4.2}$$

Using Eqs. (4.1) we obtain that

$$\begin{aligned} \Xi(\mu,\beta) &= \sum_{\{n_1,n_2,\ldots\}} \exp\left[-\beta \sum_{i=0}^{\infty} n_i\left(\varepsilon_i-\mu\right)\right] = \prod_{i=0}^{\infty}\sum_{n=0}^{\infty} \exp\left[-\beta n\left(\varepsilon_i-\mu\right)\right] \\ &= \prod_{i=0}^{\infty} \frac{1}{1-\exp\left[-\beta\left(\varepsilon_i-\mu\right)\right]}. \end{aligned} \tag{4.3}$$

Derived relation is a strict formula for partition function in the grand canonical ensemble for an ideal gas of non-interacting bosons in the one-dimensional system[4] [45].

[4] Notice that for no degeneracy of states, that expression is also correct. It is also valid for two and three-dimensional systems.

With a formula to the grand partition function, one may calculate the mean particle number in a given quantum state $\langle n_j \rangle$ and mean-square fluctuations $\sigma^2_{\langle n_j \rangle}$. For $\langle n_j \rangle$ we have

$$\begin{aligned} \langle n_j \rangle &= \frac{1}{\Xi_j} \sum_{n_j=0}^{\infty} n_j \exp\left[-\beta n_j \left(\varepsilon_j - \mu\right)\right] = \frac{\sum_{n_j=0}^{\infty} n_j x^{n_j}}{\sum_{n_j=0}^{\infty} x^{n_j}} = \frac{x \frac{d}{dx}\left(\sum_{n_j=0}^{\infty} x^{n_j}\right)}{\sum_{n_j=0}^{\infty} x^{n_j}} \\ &= \frac{1}{1/x - 1} = \frac{1}{\exp\left[\beta\left(\varepsilon_j - \mu\right)\right] - 1}, \end{aligned} \tag{4.4}$$

where Ξ_j is the sum of the single-particle state j. Mean-square fluctuations in a given quantum state may be calculated as a variance [45]

$$\sigma^2_{\langle n_j \rangle} = \langle n_j^2 \rangle - \langle n_j \rangle^2. \tag{4.5}$$

To derive $\langle n_j^2 \rangle$, we follow the same procedure as for $\langle n_j \rangle$, except that the differentiation after x must be done twice, receiving

$$\sigma^2_{\langle n_j \rangle} = \langle n_j \rangle \left[\langle n_j \rangle + 1\right] \approx \langle n_j \rangle^2. \tag{4.6}$$

This result predicts extremely high, non-physical fluctuations for a BEC ($j = 0$ state). For temperature $T = 0$ this is especially noticeable because all bosons should be in the ground state, without fluctuations. The grand canonical ensemble indicates fluctuations in order of the total number of particles, inconsistent with expectations because, at temperature $T = 0$, fluctuations should tend towards zero. Such a result is due to non-fixed particle number N. In experiments number of particles is fixed, and it is more reasonable to use the canonical ensemble for the description of the system[5]. Nevertheless, the grand canonical ensemble is remarkably useful in the present approach because it will allow us to determine the particle statistics in the canonical ensemble.

4.2. Description of an ideal Bose gas in canonical ensemble

As we mentioned previously, the canonical ensemble considers systems with fixed temperature and fixed number of particles. Therefore, it is better suited to describe experiments with ultracold atoms. The ultracold cloud is usually perfectly isolated, and there is no room for particle exchange. In the canonical ensemble, one may express the partition function of a one-dimensional system by the following expression [46]

$$Z\left(N,\beta\right) = \sum_{\{n_1,n_2,\ldots\}} \exp\left[-\beta \sum_{i=0}^{\infty} n_i \left(\varepsilon_i - \mu\right)\right] \delta_{\sum_i n_i, N}, \tag{4.7}$$

[5] Furthermore, in experiments, the energy can also be fixed, and the most appropriate ensemble for the system's description is microcanonical ensemble. However, calculations in this ensemble are still tough and challenging.

where the summation proceeds over different single-particle states' occupations. A significant difference there is the Kronecker delta, which "selects" from the particular combinations only these states for which the total number of particles in the system is N [46]. Such a notation is highly problematic, however. As it turns out, a strict analytical formula to $Z\left(N,\beta\right)$ cannot be easily provided[6]. Nevertheless, we can still provide a correct description within the canonical ensemble but using the grand canonical partition function.

There is a numerical method, which allows investigating the properties of a system in the canonical ensemble via its integral representation [46, 47]. The crucial fact is the grand partition function can be expressed by the sum of the partition functions for the canonical distribution

$$\Xi\left(\mu,\beta\right)\equiv\Xi\left(z,\beta\right)=\sum_{N=0}^{\infty}z^{N}Z\left(N,\beta\right), \tag{4.8}$$

where the substitution is such that $z=\exp\left(\beta\mu\right)$. In the formula above, the term $Z\left(N,\beta\right)$ is the partition function for the canonical ensemble with the number of particles N. That relation is extremely useful because it expresses the grand partition function as a polynomial, where $Z\left(N,\beta\right)$ is its expansion coefficient [46]. The partition function $Z\left(N,\beta\right)$ might be obtained using Cauchy's integral formula [46, 47].

Cauchy's integral formula is an essential formula from complex analysis which allows one to evaluate a contour integral of a function in the complex plane knowing its value at a singular point ξ [48]

$$f\left(\xi\right)=\frac{1}{2\pi i}\oint_{C}\frac{f(z)}{z-\xi}dz. \tag{4.9}$$

A crucial relation for our study is the n-th function derivative at ξ. The following expression follows directly from the integration by parts [48]

$$f^{(n)}\left(\xi\right)=\frac{n!}{2\pi i}\oint_{C}\frac{f(z)}{\left(z-\xi\right)^{n+1}}dz. \tag{4.10}$$

Using the relation (4.10), we can write the partition function as the integral over a closed contour from the grand partition function

$$Z\left(N,\beta\right)=\frac{1}{2\pi i}\oint_{C}\frac{\Xi\left(z,\beta\right)}{z^{N+1}}dz,\quad\Xi\left(z,\beta\right)=\prod_{i=0}^{\infty}\frac{1}{1-z\exp\left[-\beta\varepsilon_{i}\right]}, \tag{4.11}$$

with the parameter $z=\exp\left(\beta\mu\right)$. The relation (4.11) follows directly from Eq. (4.8). The integral in Eq. (4.11) is calculated following any closed contour that surrounds the zero-point in the complex plane, where the parameter z performs the function of a complex variable. The calculation of such an integral might be problematic. However, we can use the so-called saddle point method, which assumes that the partition function for a large number of particles N is mainly concentrated around its saddle point [46]. We can designate the saddle point as the integrand extremum. It is useful to write this function in the

[6] One may derive an exact analytical form of the partition function for a one-dimensional harmonic trap due to the simple form of its energy spectrum, but this is not obvious either.

exponential form

$$\begin{aligned}\frac{\Xi(z,\beta)}{z^{N+1}} &= \exp\left[\ln\frac{\Xi(z,\beta)}{z^{N+1}}\right] = \exp\left[\ln\left(\Xi(z,\beta)\right) - (N+1)\ln(z)\right] \\ &= \exp\left[-\sum_{i=0}^{\infty}\ln\left[1-z\exp\left(-\beta\varepsilon_i\right)\right] - (N+1)\ln(z)\right] = \exp\left[f(z,\beta)\right].\end{aligned} \tag{4.12}$$

A condition for the integrand extremum is an extremum of the inner exponential function

$$\frac{\partial}{\partial z}f(z,\beta) = 0 \quad \rightarrow \quad -z\frac{\partial}{\partial z}\sum_{i=0}^{\infty}\ln\left[1-z\exp\left(-\beta\varepsilon_i\right)\right] = N+1. \tag{4.13}$$

After simple transformations, we obtain the relation to the saddle point $z = z_0$

$$\sum_{i=0}^{\infty}\frac{z_0}{\exp\left(\beta\varepsilon_i\right) - z_0} - (N+1) = 0. \tag{4.14}$$

The method of calculating the integral reduces to calculating it along a contour passing exactly through $z = z_0$. For such a contour, our numerics will quickly converge. The variable z is related to a physical parameter, i.e. the chemical potential μ, so the saddle point must occur for a real value of z [46].

Having the integral form of the partition function and the equation to the saddle point, we may finally write the relations to the mean particle number $\langle n_j\rangle$ and mean-square fluctuations $\sigma^2_{\langle n_j\rangle}$ in the canonical ensemble. The mean number of particles occupying j-th energy level reads

$$\langle n_j\rangle = \frac{1}{Z(N,\beta)}\oint_C \frac{ze^{-\beta\varepsilon_j}}{1-ze^{-\beta\varepsilon_j}}\frac{\Xi(z,\beta)}{z^{N+1}}\frac{dz}{2\pi i}. \tag{4.15}$$

Fluctuations, on the other hand, are given by

$$\sigma^2_{\langle n_j\rangle} = \frac{2}{Z(N,\beta)}\oint_C \left(\frac{ze^{-\beta\varepsilon_j}}{1-ze^{-\beta\varepsilon_j}}\right)^2\frac{\Xi(z,\beta)}{z^{N+1}}\frac{dz}{2\pi i} + \langle n_j\rangle - \langle n_j\rangle^2. \tag{4.16}$$

We present the derivation of the above expressions in the appendix C.

4.3. Results of the integral method for ultracold 1D gas

To inspect the correctness of the integral method, let us consider a one-dimensional non-interacting Bose gas. Experiments over condensates are most often performed by placing the gas in magnetic or dipole traps [31, 32]. The potential of such a trap may be treated with a good approximation as the potential of a one-dimensional harmonic oscillator. The energy states of such an oscillator reads

$$\varepsilon_k = \hbar\omega\left(k+\frac{1}{2}\right) \approx \hbar\omega k, \tag{4.17}$$

where $k = 0, 1, 2, ..., \infty$. We might neglect the ground state energy because shifting the energy spectrum does not change the physical results. Note that all the formulas we have derived so far are universal. Therefore, we can apply them for different energy spectra, i.e., ε_k states, regardless of whether they are states of potential well or states of a harmonic oscillator. Firstly, we present a contour plot of the integrand module $\left|\Xi\left(z,\beta\right)/z^{N+1}\right|$ for several combinations of N values, where we have taken into account the energy spectrum of a one-dimensional harmonic trap in the grand partition function.

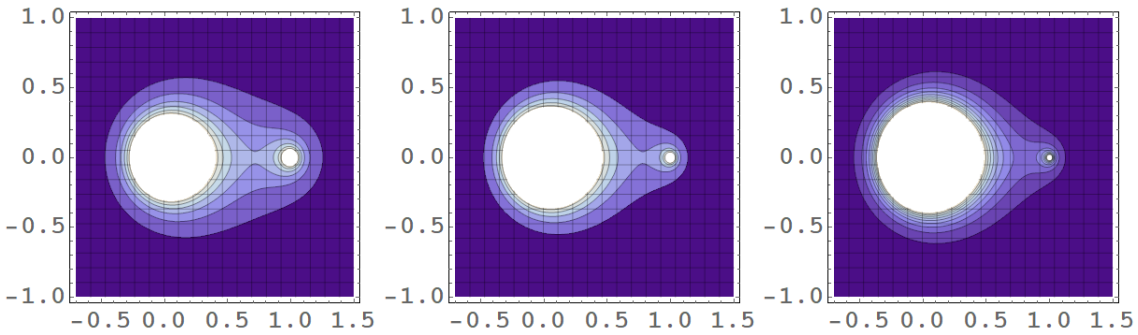

Figure 4.1. Contour plots of the integrand module $\left|\Xi\left(z,\beta\right)/z^{N+1}\right|$ for $N = 2$, $N = 3$ and $N = 4$. In the figures, we can see the characteristic saddle points located on the right-hand side of each graph. We can also see that these points are real and approximately equal to $z_0 \approx 1$.

The integral following a closed contour can be represented as the integral following a circle, using the substitution $z = z_r \exp\left(i\phi\right)$, where z_r is a real saddle point. Figure 4.2 shows values of the integrand for successive values of angle ϕ. Characteristic peaks occur around $\phi = 0$, which is when we pass precisely through the point z_r in the complex plane. It is also easy to see that the purely imaginary part does not matter in the integration process since it gives an excellent approximation to zero. This approximation for the case in Fig 4.2 is of order of 10^{-14}.

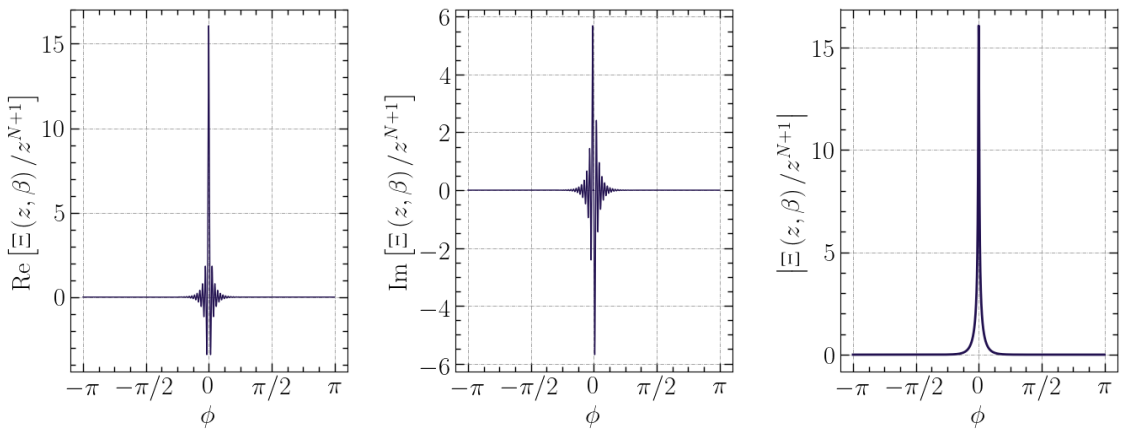

Figure 4.2. Real, imaginary and absolute values of the integrand $\Xi\left(z,\beta\right)/z^{N+1}$ for successive values of the angle ϕ for $N = 100$ particles in the condensate for temperature $5\hbar\omega/k_B$, where $\omega = 200\pi$.

Unfortunately, the phase transition leading to the Bose-Einstein condensation does not occur for one-dimensional harmonic traps. This transition appears in two- and three-dimensional systems[7]. In this case, only the degeneration of states has to be considered, and the grand partition function for the three-dimensional trap reads

$$\Xi(z,\beta) = \prod_{k=0}^{\infty} \left[\frac{1}{1 - z\exp\left[-\beta\varepsilon_k\right]} \right]^{(k+1)(k+2)/2}. \tag{4.18}$$

Below we present results for the 3D condensate using relationships (4.15) and (4.16). We see they are compatible with results obtained in literature [31, 46, 47, 49], which confirms the effectiveness of the integral method.

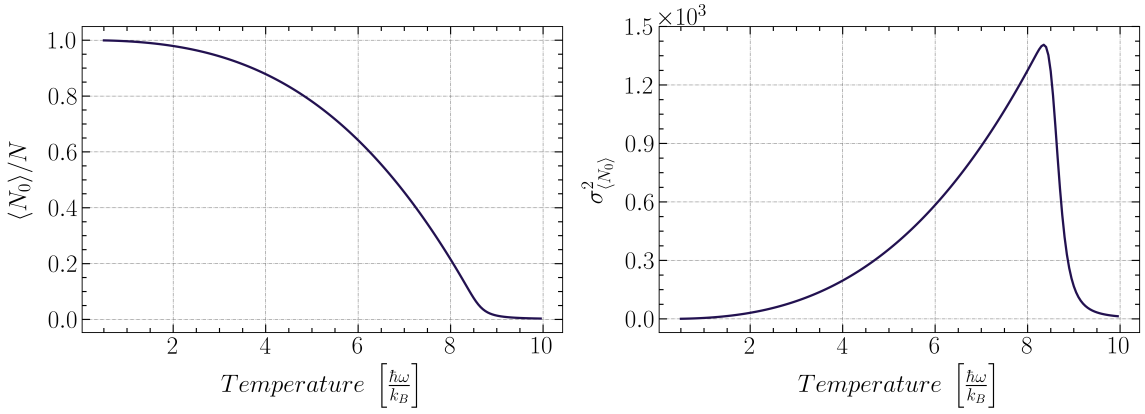

Figure 4.3. Mean particle number and mean-square fluctuations of the Bose-Einstein condensate composed of $N = 1000$ particles in the three-dimensional harmonic trap.

[7] Notice that in classical approximation, when the temperature is much greater than the differences between energy states, one may replace summation in mean particle number by integration. Then all information about the system is derived from the so-called density of energy states [1]. In the case of a box, the phase transition is possible only for 3D systems because $g(E) \sim \sqrt{E}$ and some macroscopic number of particles occupying the ground state at a fixed temperature. Considering the 3D harmonic traps, we have $g(E) \sim E^2$, meanwhile, for 2D ones, it is $g(E) \sim E$. Therefore, for both situations, the phase transition is possible.

5. Statistical properties of one-dimensional quantum droplet model

In this chapter, we propose a simple phenomenological one-dimensional quantum droplet model based on a well-known problem in quantum mechanics, i.e. the finite quantum well. We propose theoretical assumptions of the model, that is solved later. Using the energy spectrum and statistical tools derived in the previous chapter, we present the numerical results for the width of a droplet at finite temperature.

5.1. Simple phenomenological quantum droplet model

Let us recall the equations derived in the previous sections. The stationary form of the Lieb-Liniger Gross-Pitaevskii equation reads

$$\mu\,\phi(x) = \left[-\frac{\hbar^2}{2m}\frac{\partial^2}{\partial x^2} + \mu_{LL}\left[N|\phi|^2\right]\right]\phi(x) - g_{\mathrm{dd}}N\int dx'\, V^{\sigma}_{\mathrm{dd}}(x-x')|\phi(x')|^2\phi(x). \tag{5.1}$$

As we mentioned before we may rewrite the above equation to the following simple form, valid in the so-called analytical regime

$$\mu\,\phi(x) = \left[-\frac{\hbar^2}{2m}\frac{\partial^2}{\partial x^2} + \frac{\hbar^2\pi^2}{2m}N^2|\phi(x)|^4 - g_{\mathrm{dd}}N|\phi(x)|^2\right]\phi(x). \tag{5.2}$$

The stationary solution of Eq. (5.2) tends to rectangular shape as we discussed in the Section 3. Below we present another stationary solution, where the effect is even more apparent. It turns out that we can assume the rectangular ansatz as an accurate approxi-

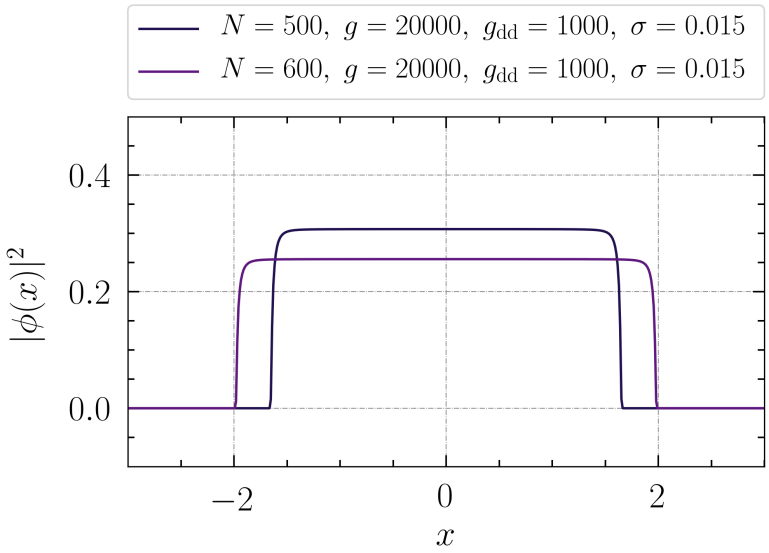

Figure 5.1. Stationary solution to the LLGPE in the quantum droplet analytical regime.

mation of the ground state [23]. One must consider that such a profile would have infinite

kinetic energy because of the sharp jump of the density at the edges. Then spatial derivatives related to the kinetic energy would tend to infinity. Nevertheless, comparing different energies before the rectangular approximation was taken, proved that kinetic energy may be neglected [23]. Regarding that, one may discard the kinetic energy from Eq. (5.2) and adopt the solution as [23]

$$\phi(x) = \frac{1}{\sqrt{W}}\mathrm{rect}\left(x/W\right), \tag{5.3}$$

where W is the quantum droplet width in the analytical regime, and the $\mathrm{rect}\left(x/W\right)$ function is defined as

$$\mathrm{rect}\left(x/W\right) = \begin{cases} 0 & \text{for} \quad W/2 < |x| < \infty, \\ 1 & \text{for} \quad |x| \leq W/2. \end{cases} \tag{5.4}$$

In order to find the best approximation of the ground state, one has to minimise the energy functional of the system with respect to W. One obtains the formula as follows [23]

$$W = \frac{2\pi^2\hbar^2}{3m}\frac{N_\mathrm{d}}{g_\mathrm{dd}}, \tag{5.5}$$

which we have already introduced in Section 3. In turn, the chemical potential is given by [23]

$$\mu = -\frac{3m}{8\pi^2\hbar^2}g_\mathrm{dd}^2. \tag{5.6}$$

Taking into account all our previous observations and rectangular ansatz of the ground state, we want to propose a simple quantum droplet model using a one-dimensional finite quantum well. Let us consider a one-dimensional closed system - quantum droplet model and its environment, composed of particles (bosons) that can occupy well-defined energy levels. These levels are: a ground state ε_0 and excited states, i.e. bound states ε_B and scattering states ε_S. At temperature $T = 0$, all particles occupy the same lowest state ε_0. With the temperature increase, these particles can move to excited states, i.e. to ε_B and ε_S states. This model assumes that the quantum droplet is formed by particles located in the ε_0 and ε_B states. The ε_0 state corresponds to a stationary droplet. The scattering states will be used to model the evaporation of particles from the droplet. Meanwhile, the ε_B states correspond to an excited droplet, e.g. perturbed by phonons. The model, as discussed later, can be improved by accounting for the correct spectrum of an excited droplet, but here we would like to study the processes of droplet evaporation only qualitatively. Therefore, we start assuming that ε_B are the energy levels in the finite quantum well with a depth V_0. The states ε_S, on the other hand, will be the scattering states. The number of particles forming a droplet N_d is a number of particles located in the ε_0 and ε_B states. We introduce the notation $W \equiv 2a$, where $2a$ is the width of a quantum well. Moreover, it is known that the chemical potential of the droplet is given by Eq. (5.6), which limits the number of available energy states. This means we can relate μ with the potential depth V_0

$$V_0 \equiv |\mu| = \frac{3m}{8\pi^2\hbar^2}g_\mathrm{dd}^2, \tag{5.7}$$

whose value determines the number of available bound states.

In the first place, we determine the energy spectrum of such a model, and then, using methods derived in Section 4, we will investigate the "droplet" evaporation.

5.2. Eigenenergies of the finite quantum well

Consider a one-dimensional quantum system in which a particle of mass m is located in a box of finite potential depth V_0 and width $2a$. This box is surrounded by an infinite potential $V = \infty$ located at a distance $\pm L$ from the origin of the coordinate system, where $|L| \gg |a|$. The infinite potential models thus a fact that the system remains closed. This situation is illustrated in Fig 5.2. The potential energy of a particle is given by the following

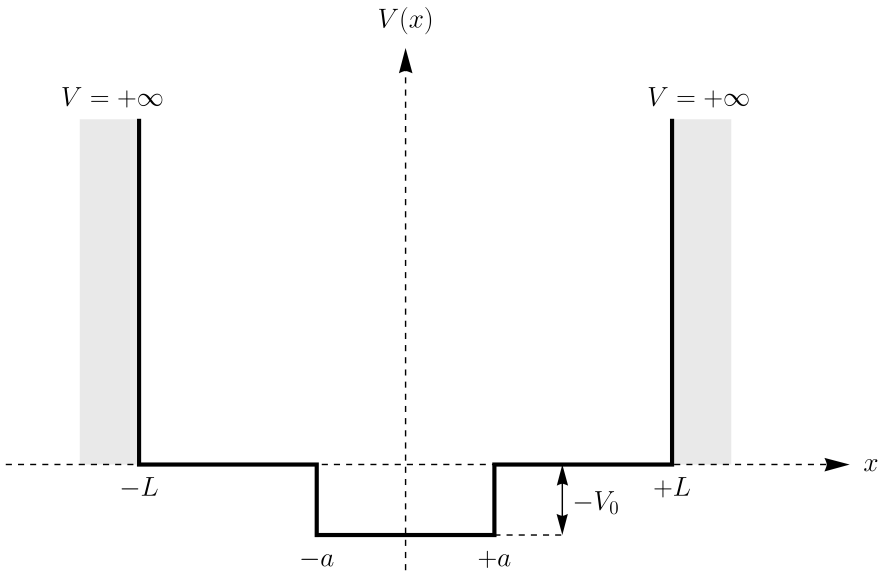

Figure 5.2. One-dimensional finite quantum well of depth V_0 and width $2a$, surrounded by an infinite potential V.

formula

$$V(x) = \begin{cases} 0 & \text{for} \quad a < |x| < L, \\ -V_0 & \text{for} \quad |x| < a, \\ \infty & \text{for} \quad |x| > L, \end{cases} \tag{5.8}$$

where we assume that the value of the parameter V_0 is positive, i.e. $V_0 > 0$. Assuming the energy of the particle E is negative, i.e. $-V_0 < E < 0$, there should be only bound energy states in the box, and their number should be finite. The particle must fulfil the stationary

Schrödinger equation

$$|x| < a: \qquad -\frac{\hbar^2}{2m}\frac{\partial^2}{\partial x^2}\psi_{\mathrm{II}}(x) - V_0\psi_{\mathrm{II}}(x) = -|E|\,\psi_{\mathrm{II}}(x), \tag{5.9}$$

$$-L < x < -a: \qquad -\frac{\hbar^2}{2m}\frac{\partial^2}{\partial x^2}\psi_{\mathrm{I}}(x) = -|E|\,\psi_{\mathrm{I}}(x), \tag{5.10}$$

$$a < x < L: \qquad -\frac{\hbar^2}{2m}\frac{\partial^2}{\partial x^2}\psi_{\mathrm{III}}(x) = -|E|\,\psi_{\mathrm{III}}(x). \tag{5.11}$$

The expression $-|E|$ takes into account the fact that the energy of a particle is negative. In addition, we introduce real and positive variables, κ and k such that

$$\kappa = \sqrt{\frac{2m}{\hbar^2}|E|}, \quad k = \sqrt{\frac{2m}{\hbar^2}\left(V_0 - |E|\right)}. \tag{5.12}$$

The wave function should: disappear at $x = -L$ and $x = L$, be continuous and has continuous derivatives at $x = -a$ and $x = a$. This gives conditions

$$\psi_{\mathrm{I}}(-L) = \psi_{\mathrm{III}}(L) = 0, \tag{5.13}$$

$$\psi_{\mathrm{I}}(-a) = \psi_{\mathrm{II}}(-a) \quad \text{and} \quad \psi_{\mathrm{II}}(a) = \psi_{\mathrm{III}}(a), \tag{5.14}$$

$$\frac{\partial}{\partial x}\psi_{\mathrm{I}}(x)\Big|_{x=-a} = \frac{\partial}{\partial x}\psi_{\mathrm{II}}(x)\Big|_{x=-a} \quad \text{and} \quad \frac{\partial}{\partial x}\psi_{\mathrm{II}}(x)\Big|_{x=a} = \frac{\partial}{\partial x}\psi_{\mathrm{III}}(x)\Big|_{x=a}. \tag{5.15}$$

Solving the problem above leads to conditions on even and odd bound energy states

$$\text{a condition for even bound states}: \quad \kappa\ \mathrm{ctgh}\left[(a-L)\,\kappa\right] = -k\ \mathrm{tg}(ka), \tag{5.16}$$

$$\text{a condition for odd bound states}: \quad \kappa\ \mathrm{ctgh}\left[(a-L)\,\kappa\right] = k\ \mathrm{ctg}(ka). \tag{5.17}$$

In a further step, one needs to analyse the allowed values of the parameters κ and k. For this purpose, we introduce the dimensionless and positive variables $\xi = ka$ and $\eta = \kappa a$. Thus we obtain the following relation

$$\xi^2 + \eta^2 = \frac{2m}{\hbar^2}V_0 a^2. \tag{5.18}$$

That is a circle equation that limits the available solutions from above. If we introduce recently defined variables into equations (5.16) and (5.17), we obtain transcendental functions of one variable (e.g., η) whose solutions determine energy states in the well. These functions read

$$\text{even}: \quad f_B(\eta) \equiv \eta\ \mathrm{ctgh}\left[\left(1-\frac{L}{a}\right)\eta\right] + \sqrt{\frac{2m}{\hbar^2}V_0 a^2 - \eta^2}\ \mathrm{tg}\sqrt{\frac{2m}{\hbar^2}V_0 a^2 - \eta^2} = 0, \tag{5.19}$$

$$\text{odd}: \quad f_B(\eta) \equiv \eta\ \mathrm{ctgh}\left[\left(1-\frac{L}{a}\right)\eta\right] - \sqrt{\frac{2m}{\hbar^2}V_0 a^2 - \eta^2}\ \mathrm{ctg}\sqrt{\frac{2m}{\hbar^2}V_0 a^2 - \eta^2} = 0. \tag{5.20}$$

The energies of each state are given by the following formula and stem from the relation $\eta = \kappa a$

$$\varepsilon_B \equiv \varepsilon_B(\eta, a) = -\frac{\hbar^2 \eta^2}{2ma^2}, \tag{5.21}$$

where η behaves like an iterator and represents successive solutions of the equations (5.19) and (5.20). The number of solutions to these equations is finite, and it follows that the number of bound states in the well is limited. Looking for solutions is therefore restricted to the range $\eta \in (0, \lambda)$, where λ is given by the expression below

$$\lambda \equiv \lambda(V_0, a) = \sqrt{\frac{2m}{\hbar^2} V_0 a^2}. \tag{5.22}$$

We perform analogous considerations for scattering levels. In this case, the particle must again satisfy a similar, though slightly different, Schrödinger equation

$$|x| < a: \qquad -\frac{\hbar^2}{2m}\frac{\partial^2}{\partial x^2}\psi_{\mathrm{II}}(x) - V_0\psi_{\mathrm{II}}(x) = E\,\psi_{\mathrm{II}}(x), \tag{5.23}$$

$$-L < x < -a: \qquad -\frac{\hbar^2}{2m}\frac{\partial^2}{\partial x^2}\psi_{\mathrm{I}}(x) = E\,\psi_{\mathrm{I}}(x), \tag{5.24}$$

$$a < x < L: \qquad -\frac{\hbar^2}{2m}\frac{\partial^2}{\partial x^2}\psi_{\mathrm{III}}(x) = E\,\psi_{\mathrm{III}}(x). \tag{5.25}$$

In this situation the energy of the particle is positive i.e. $E > 0$. As before, we introduce the positive and real variables κ and k

$$\kappa = \sqrt{\frac{2m}{\hbar^2}E}, \quad k = \sqrt{\frac{2m}{\hbar^2}(V_0 + E)}. \tag{5.26}$$

The wave function $\psi(x)$ must satisfy the same boundary conditions i.e. (5.13), (5.14) and (5.15). In this way, we derive equations whose solutions describe the successive scattering states

$$\text{even}: \quad f_S(\eta) \equiv \eta\ \mathrm{ctg}\left[\left(1 - \frac{L}{a}\right)\eta\right] + \sqrt{\frac{2m}{\hbar^2}V_0 a^2 + \eta^2}\ \mathrm{tg}\sqrt{\frac{2m}{\hbar^2}V_0 a^2 + \eta^2} = 0, \tag{5.27}$$

$$\text{odd}: \quad f_S(\eta) \equiv \eta\ \mathrm{ctg}\left[\left(1 - \frac{L}{a}\right)\eta\right] - \sqrt{\frac{2m}{\hbar^2}V_0 a^2 + \eta^2}\ \mathrm{ctg}\sqrt{\frac{2m}{\hbar^2}V_0 a^2 + \eta^2} = 0. \tag{5.28}$$

Energies of scattering states are given by the following expression

$$\varepsilon_S \equiv \varepsilon_S(\eta, a) = \frac{\hbar^2 \eta^2}{2ma^2}. \tag{5.29}$$

The scattering levels are not limited by any condition, so we are looking for solutions to the equations (5.27) and (5.28) in the range $\eta \in (0, \infty)$.

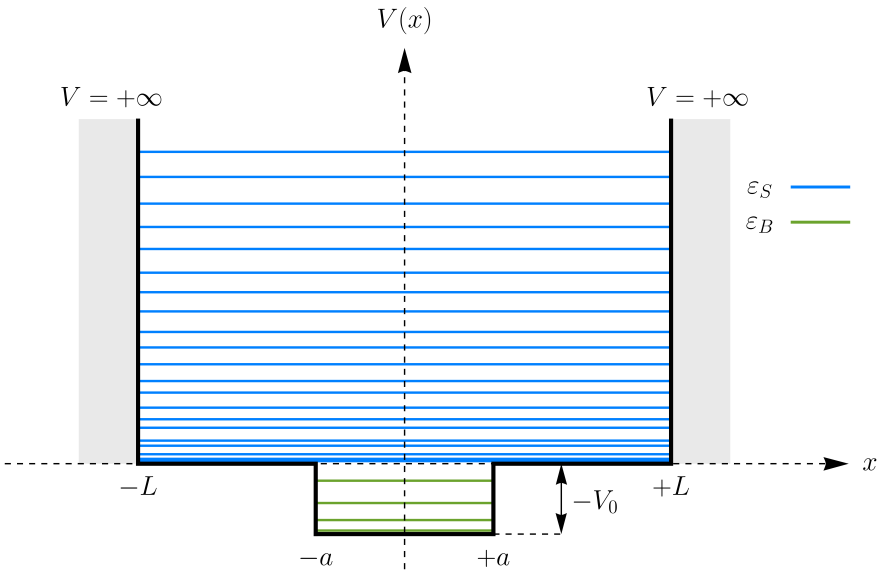

Figure 5.3. Example placement of energy states, based on solutions to the equations (5.19), (5.20), (5.27) and (5.28).

5.3. Evaporation of droplet – numerical results

The quantum well eigenenergies ε_B, ε_S, and the additional lowest-lying state ε_0, permit us to build particle statistics based on statistical ensembles, which allows studying the mean particle number of each state and thus the width of the quantum droplet as a function of temperature T. In order to do this, we use the formula (5.5). The number of particles N_d which create a quantum droplet is the mean number of particles that occupy the corresponding energy states of the finite quantum well. We can therefore write that N_d is expressed as follows

$$N_\mathrm{d} = \langle n_0 \rangle + \langle n_B \rangle, \tag{5.30}$$

where $\langle n_0 \rangle$ is the mean particle number located in the ground state and $\langle n_B \rangle$ is the mean number of particles located in all bound states. Therefore, we determine W as

$$W = \frac{2\pi^2\hbar^2}{3m}\frac{N_\mathrm{d}}{g_\mathrm{dd}} = \frac{2\pi^2\hbar^2}{3m}\frac{\langle n_0 \rangle + \langle n_B \rangle}{g_\mathrm{dd}}, \tag{5.31}$$

using the integral formula (4.15)[8] As the temperature T increases, the average occupation of each energy state changes. If the temperature reaches a value for which some of the particles go to the scattering states ε_S, the droplet width W and thus the energy spectrum will change. This means that the so-called self-consistent calculation has to be applied.

[8] Notice that we calculate only mean particle number in specific quantum well states. We do not evaluate mean-square fluctuations because it turns out that the integral formula does not consider the correlations between levels. That fluctuations formula correctly describes only one state, which is consistent with results derived for BEC because we investigate only the ground state there. One cannot just add up fluctuations for each state that create the droplet because the result is not physical. However, we may do this for ordinary occupations.

This calculus means that we determine the energy spectrum at a fixed temperature T and then calculate the width W. Then, to stabilise the droplet at this temperature, we again determine the energy spectrum and the width. We can name this process "thermalisation" of the droplet. In the simulation, we assumed five steps of thermalisation[9] and the total width of the system is equal to $2L = 12\ l$. In addition, we shifted the entire energy spectrum by the potential depth V_0. Such an operation does not affect the physical results but significantly simplifies the numerical calculations. Therefore, we suppose that $\varepsilon_0 = 0$.

Moreover, we may use a real energy spectrum for droplets derived from the assumption of a rectangular ansatz of its density profile. It turns out that the bound spectrum can be represented as [23]

$$\varepsilon_B^k = \left(\frac{3}{2\pi}\right)^2 \frac{m}{\hbar^2} \frac{g_{\mathrm{dd}}^2 k}{N_{\mathrm{d}}} \sqrt{\frac{1}{3} + \frac{k^2}{4N_{\mathrm{d}}^2}}, \tag{5.32}$$

where $k = 1, 2, 3, \ldots$ iterates the successive energy states. The number of available levels is limited by the chemical potential μ, i.e. $\varepsilon_B^{k_{max}} = |\mu|$ [23], which is equivalent to the parameter V_0. As before, we take $\varepsilon_0 = 0$ as the ground state, while for the scattering states ε_S we propose the following expression

$$\varepsilon_S^k = \frac{\hbar^2}{2m}\left(\frac{\pi k}{L}\right)^2 + V_0, \tag{5.33}$$

where the variable k iterates successive scattering levels. In the following, we present the results of quantum droplet width as a function of temperature based on the quantum well and actual energy spectra.

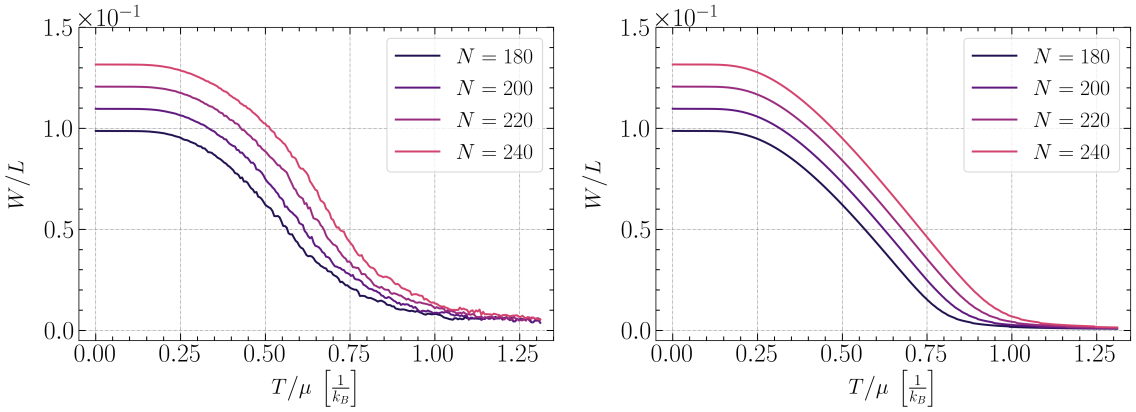

Figure 5.4. Width of the quantum droplet as a function of temperature T, based on the finite quantum well (left panel) and actual (right panel) spectrum. In both cases, the dipolar coupling constant equals $g_{\mathrm{dd}} = 1000$.

In Fig. 5.4, we can see that the evaporation process is similar in both cases. Initially, the width of the quantum droplet is constant. It is related to the assumption that the

[9] This is an arbitrary value. During the simulation, we have seen that the droplet usually stabilises after about 2-4 steps.

droplet is composed of particles located in bound states. Initially, the temperature is too low, and there are no particles in the scattering states. However, the consistent increase of temperature causes some particles to move to these states, and the droplet starts shrinking. We also see that none of the droplets evaporates slower or faster. The processes are similar for the same dipolar coupling constant, which is especially visible in the case of the actual energy spectrum. One may see that the evaporation profiles for droplets built from the finite quantum well spectrum are a little ragged. That is probably because the energy spectrum in each step is calculated numerically. Moreover, the self-consistent calculation perhaps cannot stabilise the droplet, and the number of energy states jumps between different values, affecting the number of bound states and droplet width. For the actual energy spectrum, we have the exact formula for eigenenergies. Thus, the profiles do not have any jumps and are smooth even at high temperatures.

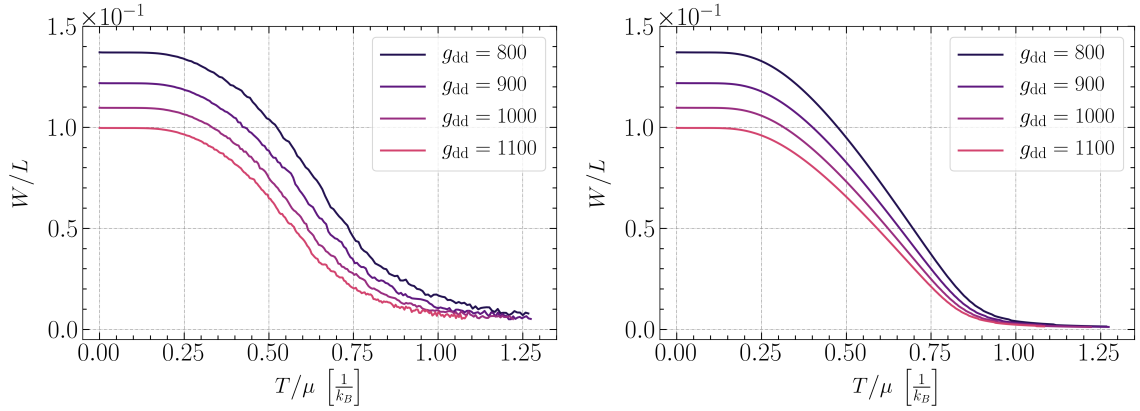

Figure 5.5. Width of the quantum droplet as a function of temperature T, based on the finite quantum well (left panel) and actual (right panel) spectrum. In both cases, the total number of particles in the system equals $N = 200$.

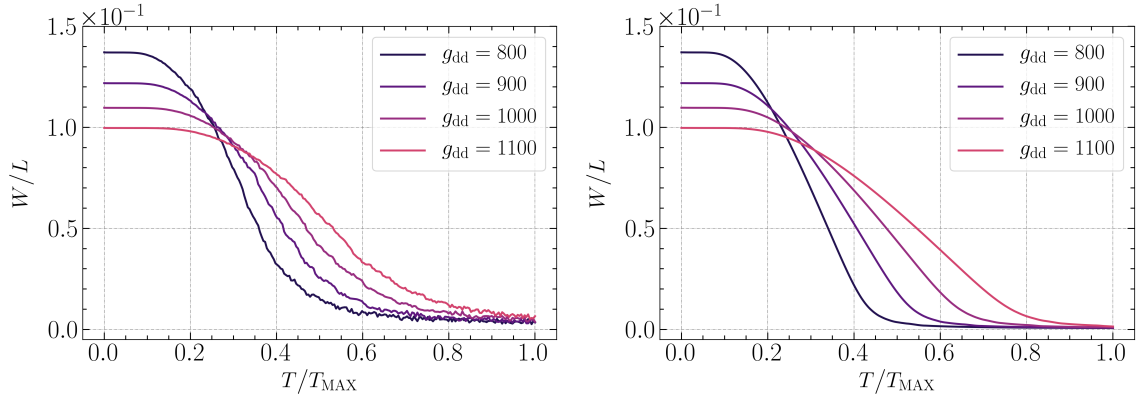

Figure 5.6. The same case as in Fig. 5.5, but in different units. T_{MAX} denotes the maximal temperature used during simulations.

In Fig. 5.5 we see the evaporation profiles are highly similar to the previous cases, but there are different dipolar coupling constants, that modify the chemical potential μ.

Therefore, it is good to present profiles in other units. In Fig. 5.6 one can see the droplet shrinks faster for lower values of dipolar coupling constant. That could mean as the dipole interaction becomes stronger, the droplet is less eager to evaporate. Such a situation seems possible. Notice that the dipolar interaction is attractive. Therefore, the greater the dipolar coupling constant, the stronger particles attract each other. That means one has to use more energy to separate particles from the droplet, which is related to providing higher temperatures. From the perspective of the finite quantum well, it means there are more bound states, by which one has to provide a higher temperature to allow particles to escape to scattering states.

To sum up, we see that the proposed quantum droplet model in the form of a finite quantum well has a similar evaporation profile to the actual spectrum found in [23]. We believe that the proposed model correctly describes one-dimensional quantum droplet evaporation in the analytical regime.

6. Summary

This thesis has aimed to investigate several properties of one-dimensional quantum droplets. These new ultra-dilute forms could arise in both Bose-Bose mixtures, predicted by D. Petrov [13] and in one-component Bose systems with a substantial magnetic moment, as predicted by A. Pelster [50] and observed by T. Pfau's group [12].

In order to study quantum droplets, we used the Lieb-Liniger Gross-Pitaevskii equation (LLGPE) extended by the dipolar interaction term [24]. To better understand the LLGPE, in Section 2 we initially recalled the basics of many-body quantum mechanics for bosonic systems. We derived the well-known Gross-Pitaevskii equation (GPE) for weak, short-range interactions, using the second quantisation formalism and mean-field approximation theory [1, 31]. The latter equation has gained its popularity foremost for an approximate description of the weakly-interacting Bose system, including low-energy excitations and solitons [33]. However, even in a weakly-interacting regime, the GPE does not describe such exciting phenomena as quantum depletion [34, 35]. During the thesis, we focused on strongly interacting particles, for which the GPE does not provide the correct description. To derive the appropriate equation, which respects such a regime, we used the exact solution found by E. Lieb [29, 30]. That model allows the investigation of homogeneous one-dimensional gas for any strength of short-range interaction, in the effective form such as $V\left(x-x'\right)=g\delta\left(x-x'\right)$. However, solutions from the LL model are not handy and are usually studied only for a small number of particles (of the order of several). Therefore, we introduced the appropriate equation with non-linear Lieb-Liniger chemical potential μ_{LL}, using the hydrodynamic approach [25, 26]. Such an equation gives reliable results for strong interactions [41]. In [24] the equation was extended to the gas with strong short-range repulsion and weak dipolar attraction to show the existence of one-dimensional quantum dipolar droplets.

Subsequently, in Section 3 we focused on the stationary form of the LLGPE. That equation offers several types of solutions. Primarily there are bright solitons [41] and quantum droplets [23, 24]. There is also the so-called analytical regime of quantum droplets (fermionised quantum droplets) where the analytical solution is known [23]. That regime corresponds to weak and short-range effective dipolar interaction with $\sigma \to 0$ and strong short-range interaction $g \to \infty$. In such a regime the stationary LLGPE take a significantly simpler form. Our objective was to investigate what happens with the fermionised quantum droplet in real-time in the case when we perturbed its stationary solution. During simulations, it turned out that when we prepared a system with additional energy in the form of noise, the dynamic of a perturbed quantum droplet is highly complex. Several particles leave a droplet, and the droplet first shrinks and then it stabilises. We conducted many simulations with perturbed systems, adding energy in different ways, i.e. by deterministic and random functions. We noted that the result depends only on the amount of the added energy but not the method of adding the perturbations. Taking into account our observations, in the subsequent section, we proposed a simple phenomenological model

of a quantum droplet, which allowed us to study its statistical properties. However, before that, we presented the basics of statistical ensembles, which provided us with appropriate numerical tools to investigate the evaporation of droplets.

Thus, in Section 4, we thoroughly analysed the statistical ensembles to find a proper description of the mean particle number in any quantum state [45]. In order to do so, we used the canonical ensemble that adequately describes systems with a fixed number of particles [45]. Unfortunately, the explicit representation of the partition function in the canonical ensemble is hampered by the Kronecker delta, which ensures a constant number of particles in the system. Therefore, we have used the numerical method of representing the partition function as a contour integral from the grand partition function in the complex plane [46, 47]. Having the formula to $Z(N,\beta)$, we presented integral formulas that allowed us to determine the mean particle number of the individual energy states in the canonical ensemble. In addition, we considered an equation for the so-called saddle point, used in efficient calculation of the contour integral [46]. For illustration, we presented a short description of the Bose-Einstein condensate and well-studied results of such a system [31, 32].

Finally, we proposed a phenomenological one-dimensional quantum droplet model in the last Section. In that section, we again recalled the stationary form of the LLGPE. The LLGPE solutions we investigated in the analytical regime resemble rectangular shapes with reasonable accuracy. Moreover, the kinetic energy of these systems is minimal compared to the interaction energies. Accordingly, one may neglect the kinetic term and take the solution as the rectangular ansatz [23]. Making such an assumption results in the wave function being described by only one parameter - the quantum droplet width W, which in turn, in the adopted regime, depends only on the particle number N_{d} and dipolar coupling constant g_{dd}. Because of our observations and rectangular ansatz with the W parameter, we built the quantum droplet model based on a finite quantum well. The finite quantum well is a simple problem in quantum mechanics, but despite its simplicity, one can only find its eigenenergies numerically. Nevertheless, having the energy spectrum of it and tools derived in Section 4, we could investigate the droplet's evaporation under heating. We compared these results with results obtained from the exact energy spectrum of a quantum droplet in the analytical regime. These results were very similar, but due to the numerical determination of the quantum well spectrum, the droplet width profile was a little ragged. We observe that the larger the dipolar coupling constant increase, the slower is droplet evaporation. From the perspective of quantum well, it is related to a larger number of bound states, by which the particles escape to the scattering state at a higher temperature.

The thesis leads to several research problems which we did not undertake. Primarily one may compare the results obtained from the quantum droplet model and direct from the LLGPE. For this purpose, one must conduct many simulations with different added energies to the system. These results are obtained in the microcanonical ensemble. Therefore, one needs to transfer these to the canonical one and ensure the same boundary

conditions in both methods earlier. The second problem is determining the mean-square fluctuations of particles in the droplet model. The equation we provided is correct only for investigating individual states. Thereby it gives excellent results for the ground state of typical BEC systems. However, that formula does not take into account multilevel correlations. Therefore, in the case of the quantum droplet model, which is composed of particles located in different quantum states, simply adding up the fluctuations for individual levels is not physical. Another problem we did not discuss is that one may continue with the numerical calculus of the partition function in canonical ensemble and the saddle point, which finally should lead to the Gaussian integral. It should allow for to investigation of larger systems more efficiently.

A. Accurate approximation form of $e_{LL}(\gamma)$

Calculation of the Lieb-Liniger chemical potential requires knowing embedded function $e_{\mathrm{LL}}(\gamma)$. Fortunately, this function has an accurate and comprehensive polynomial form derived as a numerical approximation [36]. For weak interactions $\gamma < 1$, we have

$$e_{\mathrm{LL}}(\gamma) \approx \gamma - \frac{4}{3\pi}\gamma^{3/2} + \left[\frac{1}{6} - \frac{1}{\pi^2}\right]\gamma^2 - 0.0016\gamma^{5/2} + \mathcal{O}\left(\gamma^3\right). \tag{A.1}$$

In the region of intermediate forces $1 \leq \gamma < 15$, approximation reads

$$\begin{aligned} e_{\mathrm{LL}}(\gamma) \approx \gamma - \frac{4}{3\pi}\gamma^{3/2} + \left[\frac{1}{6} - \frac{1}{\pi^2}\right]\gamma^2 - 0.002005\gamma^{5/2} + 0.000419\gamma^3 - \\ 0.000284\gamma^{7/2} + 0.000031\gamma^4. \end{aligned} \tag{A.2}$$

Whereas for strong interactions $\gamma \geq 15$, as follows

$$\begin{aligned} e_{\mathrm{LL}}(\gamma) \approx \frac{\pi^2}{3}\Bigg[1 - \frac{4}{\gamma} + \frac{12}{\gamma^2} - \frac{10.9448}{\gamma^3} - \frac{130.552}{\gamma^4} + \frac{804.13}{\gamma^5} - \frac{910.345}{\gamma^6} - \frac{15423.8}{\gamma^7} + \\ \frac{100559.0}{\gamma^8} - \frac{67110.5}{\gamma^9} - \frac{2.64681\cdot 10^6}{\gamma^{10}} + \frac{1.55627\cdot 10^7}{\gamma^{11}} + \frac{4.69185\cdot 10^6}{\gamma^{12}} - \\ \frac{5.35057\cdot 10^8}{\gamma^{13}} + \frac{2.6096\cdot 10^9}{\gamma^{14}} + \frac{4.84076\cdot 10^9}{\gamma^{15}} - \frac{1.16548\cdot 10^{11}}{\gamma^{16}} + \frac{4.35667\cdot 10^{11}}{\gamma^{17}} + \\ \frac{1.93421\cdot 10^{12}}{\gamma^{18}} - \frac{2.60894\cdot 10^{13}}{\gamma^{19}} + \frac{6.51416\cdot 10^{13}}{\gamma^{20}} + \mathcal{O}\left(\frac{1}{\gamma^{21}}\right)\Bigg]. \end{aligned} \tag{A.3}$$

B. Hydrodynamical approach for LLGPE

In order to provide hydrodynamical approach we insert complex function (2.19) with its condition to the LLGPE (2.20). During the proof we will omit the arguments of $\rho(x,t)$, $v(x,t)$, $\varphi(x,t)$ and $\phi(x,t)$ for clarity of calculations, having their dependence of position and time in mind. Let us recollect these relationships

$$i\hbar\frac{\partial}{\partial t}\phi = -\frac{\hbar^2}{2m}\frac{\partial^2}{\partial x^2}\phi + \mu_{LL}\left[N\left|\phi\right|^2\right]\phi, \quad \phi = \sqrt{\frac{\rho}{N}}e^{i\varphi}, \quad \frac{\hbar}{m}\frac{\partial\varphi}{\partial x} = v. \tag{B.1}$$

Therefore, we have

$$i\hbar\frac{\partial}{\partial t}\sqrt{\frac{\rho}{N}}e^{i\varphi} + \frac{\hbar^2}{2m}\frac{\partial^2}{\partial x^2}\sqrt{\frac{\rho}{N}}e^{i\varphi} - \mu_{LL}\left[\rho\right]\sqrt{\frac{\rho}{N}}e^{i\varphi} = 0. \tag{B.2}$$

Now, we calculate appropriate derivatives, next we put these forms to (B.2) and simplify the constants. In this way, we get equation with real and imaginary terms

$$\begin{aligned}&\mathscr{R}\left[-\mu_{\mathrm{LL}}[\rho] - \hbar\frac{\partial\varphi}{\partial t} - \frac{\hbar^2}{2m}\left(\frac{\partial\varphi}{\partial x}\right)^2 - \frac{\hbar^2}{8m\rho^2}\left(\frac{\partial\rho}{\partial x}\right)^2 + \frac{\hbar^2}{4m\rho}\frac{\partial^2\rho}{\partial x^2}\right] + \\ &i\mathscr{I}\left[-\frac{\hbar}{2\rho}\frac{\partial\rho}{\partial t} - \frac{\hbar^2}{2m\rho}\frac{\partial\rho}{\partial x}\frac{\partial\varphi}{\partial x} - \frac{\hbar^2}{2m}\frac{\partial^2\varphi}{\partial x^2}\right] = 0.\end{aligned} \tag{B.3}$$

Let us consider the imaginary part. We multiply this expression by $\left(-2m\rho/\hbar\right)$ and get

$$m\frac{\partial\rho}{\partial t} + \hbar\frac{\partial\rho}{\partial x}\frac{\partial\varphi}{\partial x} + \hbar\rho\frac{\partial^2\varphi}{\partial x^2} = 0. \tag{B.4}$$

Next, we use the relation that $\partial\varphi/\partial x = mv/\hbar$

$$\frac{\partial\rho}{\partial t} + v\frac{\partial\rho}{\partial x} + \rho\frac{\partial v}{\partial x} = 0. \tag{B.5}$$

In this way, we see that we obtained the continuity equation

$$\frac{\partial}{\partial t}\rho + \frac{\partial}{\partial x}\left(\rho v\right) = 0. \tag{B.6}$$

It remains to consider the real part. Let us take into account only its first three terms and compare these to zero

$$-\mu_{\mathrm{LL}}\left[\rho\right] - \hbar\frac{\partial\varphi}{\partial t} - \frac{\hbar^2}{2m}\left(\frac{\partial\varphi}{\partial x}\right)^2 = 0. \tag{B.7}$$

Now we act on this equation with the differentiate operator over x

$$\hbar\frac{\partial}{\partial t}\frac{\partial\varphi}{\partial x} + \frac{\hbar^2}{2m}\frac{\partial}{\partial x}\left(\frac{\partial\varphi}{\partial x}\right)^2 = -\frac{\partial}{\partial x}\mu_{\mathrm{LL}}\left[\rho\right]. \tag{B.8}$$

We again use the relationship that $\partial\varphi/\partial x = mv/\hbar$ and we obtain

$$\frac{\partial}{\partial t}v + v\frac{\partial}{\partial x}v = -\frac{1}{m}\frac{\partial}{\partial x}\mu_{\mathrm{LL}}\left[\rho\right], \tag{B.9}$$

which is the Euler equation. Remains the question, what are the other two terms in the real part of (B.3). It turns out it is the so-called quantum pressure which may be neglected that we mentioned in the main part of the thesis. That pressure is defined in the following way [26]

$$Q = -\frac{\hbar^2}{2m}\frac{1}{\sqrt{\rho}}\frac{\partial^2\sqrt{\rho}}{\partial x^2}. \tag{B.10}$$

Calculate the second derivative gives expression as follows

$$-\frac{\hbar^2}{2m}\frac{1}{\sqrt{\rho}}\frac{\partial^2\sqrt{\rho}}{\partial x^2} = \frac{\hbar^2}{8m\rho^2}\left(\frac{\partial\rho}{\partial x}\right)^2 - \frac{\hbar^2}{4m\rho}\frac{\partial^2\rho}{\partial x^2}, \tag{B.11}$$

which are the same parts as in (B.3).

C. Derivation of $\langle n_j \rangle$ and $\sigma^2_{\langle n_j \rangle}$

We can express the mean particle number in the state j by an appropriate derivative from the partition function [45]

$$\langle n_j \rangle = -\frac{1}{\beta}\frac{\partial}{\partial \varepsilon_j}\ln\left[Z\left(N,\beta\right)\right] = -\frac{1}{\beta}\frac{1}{Z\left(N,\beta\right)}\frac{\partial}{\partial \varepsilon_j}Z\left(N,\beta\right). \tag{C.1}$$

Now, in place of the differentiation of partition function, we insert its integral representation

$$\langle n_j \rangle = -\frac{1}{\beta}\frac{1}{Z\left(N,\beta\right)}\frac{\partial}{\partial \varepsilon_j}\oint_C \frac{\Xi\left(z,\beta\right)}{z^{N+1}}\frac{dz}{2\pi i}. \tag{C.2}$$

In place of the grand partition function, we insert its analytical formula and move the differentiation under the integral

$$\langle n_j \rangle = -\frac{1}{\beta}\frac{1}{Z\left(N,\beta\right)}\oint_C \frac{dz}{2\pi i}\frac{1}{z^{N+1}}\frac{\partial}{\partial \varepsilon_j}\prod_{i=0}^{\infty}\frac{1}{1-ze^{-\beta\varepsilon_i}}. \tag{C.3}$$

In general, the derivative of a product is defined as

$$\frac{d}{dx}\prod_{i=0}^{k} f_i(x) = \left(\prod_{i=0}^{k} f_i(x)\right)\left(\sum_{i=0}^{k}\frac{f_i'(x)}{f_i(x)}\right). \tag{C.4}$$

In our case, we differentiate with respect to only one term, i.e. ε_j. This means that from the whole sum, only the derivative of the element containing ε_j, divided by this element, will remain. Thus, we obtain

$$\langle n_j \rangle = -\frac{1}{\beta}\frac{1}{Z\left(N,\beta\right)}\oint_C \frac{dz}{2\pi i}\frac{\Xi\left(z,\beta\right)}{z^{N+1}}\frac{-\beta z e^{-\beta\varepsilon_j}}{\left(1-ze^{-\beta\varepsilon_j}\right)^2}\left(1-ze^{-\beta\varepsilon_j}\right). \tag{C.5}$$

Finally, the formula for $\langle n_j \rangle$ reduces to the following form

$$\langle n_j \rangle = \frac{1}{Z\left(N,\beta\right)}\oint_C \frac{ze^{-\beta\varepsilon_j}}{1-ze^{-\beta\varepsilon_j}}\frac{\Xi\left(z,\beta\right)}{z^{N+1}}\frac{dz}{2\pi i}. \tag{C.6}$$

The mean-square fluctuations $\sigma^2_{\langle n_j \rangle}$ can be determined by doing differentiation twice [45]

$$\begin{aligned}\sigma^2_{\langle n_j \rangle} &= \frac{1}{\beta^2}\frac{\partial}{\partial \varepsilon_j}\left[\frac{\partial}{\partial \varepsilon_j}\ln\left[Z\left(N,\beta\right)\right]\right] = \frac{1}{\beta^2}\frac{\partial}{\partial \varepsilon_j}\left[\frac{1}{Z\left(N,\beta\right)}\frac{\partial}{\partial \varepsilon_j}Z\left(N,\beta\right)\right] \\ &= \frac{1}{\beta^2}\left[-\left(\frac{1}{Z\left(N,\beta\right)}\right)^2\frac{\partial}{\partial \varepsilon_j}Z\left(N,\beta\right)\frac{\partial}{\partial \varepsilon_j}Z\left(N,\beta\right) + \frac{1}{Z\left(N,\beta\right)}\frac{\partial^2}{\partial \varepsilon_j^2}Z\left(N,\beta\right)\right].\end{aligned} \tag{C.7}$$

It is easy to observe that the first term is the square of the mean particle number

$$\sigma^2_{\langle n_j \rangle} = -\langle n_j \rangle^2 + \frac{1}{\beta^2} \frac{1}{Z\left(N,\beta\right)} \frac{\partial^2}{\partial \varepsilon_j^2} Z\left(N,\beta\right). \tag{C.8}$$

This leaves the second term to be determined. During the calculation, we can omit the constants in order to simplify the notation

$$\frac{\partial^2}{\partial \varepsilon_j^2} Z\left(N,\beta\right) = \frac{\partial}{\partial \varepsilon_j} \left[\frac{\partial}{\partial \varepsilon_j} Z\left(N,\beta\right) \right] = \frac{\partial}{\partial \varepsilon_j} \left[\frac{\partial}{\partial \varepsilon_j} \oint_C \frac{\Xi\left(z,\beta\right)}{z^{N+1}} \frac{dz}{2\pi i} \right]. \tag{C.9}$$

We use the previously determined expression for the derivative in parentheses

$$\begin{aligned} \frac{\partial^2}{\partial \varepsilon_j^2} Z\left(N,\beta\right) &= \frac{\partial}{\partial \varepsilon_j} \left[\oint_C \frac{-\beta z e^{-\beta\varepsilon_j}}{1 - z e^{-\beta\varepsilon_j}} \frac{\Xi\left(z,\beta\right)}{z^{N+1}} \frac{dz}{2\pi i} \right] \\ &= \oint_C \frac{dz}{2\pi i} \frac{1}{z^{N+1}} \frac{\partial}{\partial \varepsilon_j} \left(\frac{-\beta z e^{-\beta\varepsilon_j}}{1 - z e^{-\beta\varepsilon_j}} \Xi\left(z,\beta\right) \right). \end{aligned} \tag{C.10}$$

The derivative under the integral is equal to

$$\frac{\beta^2 \left(z e^{-\beta\varepsilon_j}\right)^2}{\left(1 - z e^{-\beta\varepsilon_j}\right)^2} \Xi\left(z,\beta\right) + \frac{\beta^2 z e^{-\beta\varepsilon_j}}{1 - z e^{-\beta\varepsilon_j}} \Xi\left(z,\beta\right) - \frac{\beta z e^{-\beta\varepsilon_j}}{1 - z e^{-\beta\varepsilon_j}} \frac{\partial}{\partial \varepsilon_j} \Xi\left(z,\beta\right). \tag{C.11}$$

When the last expression is differentiated, it will be equal to the first one, so in total, these parts will add up. The expression in the middle is, in turn, equivalent to the mean particle number $\langle n_j \rangle$. If we put everything together keeping in mind the constants, we get the formula for the fluctuations of the j-th state

$$\sigma^2_{\langle n_j \rangle} = \frac{2}{Z\left(N,\beta\right)} \oint_C \left(\frac{z e^{-\beta\varepsilon_j}}{1 - z e^{-\beta\varepsilon_j}} \right)^2 \frac{\Xi\left(z,\beta\right)}{z^{N+1}} \frac{dz}{2\pi i} + \langle n_j \rangle - \langle n_j \rangle^2. \tag{C.12}$$

D. Software implementation

The code implementation of the Lieb-Liniger Gross-Pitaevskii equation, imaginary-time and real-time evolution methods is available at https://gitlab.com/jakkop/mudge. I did not contribute to the code implementation in any way. I only used it during the thesis by modifying the added noise and parameters.

The code implementation of the droplet model and integral path method is available at https://github.com/mateuszk098/Droplet-Model. It is entirely my work.

References

[1] Sacha, K. *Kondensat Bosego Einsteina* (Instytut Fizyki im. M. Smoluchowskiego, Kraków, Uniwersytet Jagielloński, 2004).

[2] Metcalf, H. & van der Straten, P. *Laser Cooling and Trapping*. Journal of the Optical Society of America B **20** (2003).

[3] Anderson, M. H., Ensher, J. R., Matthews, M. R., Wieman, C. E. & Cornell, E. A. *Observation of Bose-Einstein condensation in a dilute atomic vapor*. Science **269,** 198–201 (1995).

[4] Davis, K. B. *et al. Bose-Einstein condensation in a gas of sodium atoms*. Phys. Rev. Lett. **75,** 3969–3973 (1995).

[5] Bradley, C. C., Sackett, C. A., Tollett, J. J. & Hulet, R. G. *Evidence of Bose-Einstein Condensation in an Atomic Gas with Attractive Interactions*. Phys. Rev. Lett. **75,** 1687–1690 (1995).

[6] Chin, C., Grimm, R., Julienne, P. & Tiesinga, E. *Feshbach resonances in ultracold gases*. Rev. Mod. Phys. **82,** 1225–1286 (2010).

[7] Inouye, S. *et al. Observation of Feshbach resonances in a Bose–Einstein condensate*. Nature **392,** 151–154 (1998).

[8] Góral, K., Rzążewski, K. & Pfau, T. *Bose-Einstein condensation with magnetic dipole-dipole forces*. Physical Review A **61** (2000).

[9] Santos, L., Shlyapnikov, G. V., Zoller, P. & Lewenstein, M. *Bose-Einstein Condensation in Trapped Dipolar Gases*. Phys. Rev. Lett. **85,** 1791–1794 (2000).

[10] Griesmaier, A., Werner, J., Hensler, S., Stuhler, J. & Pfau, T. *Bose-Einstein Condensation of Chromium*. Phys. Rev. Lett. **94,** 160401 (2005).

[11] Lahaye, T., Menotti, C., Santos, L., Lewenstein, M. & Pfau, T. *The physics of dipolar bosonic quantum gases*. Reports on Progress in Physics **72,** 126401 (2009).

[12] Kadau, H. *et al. Observing the Rosensweig instability of a quantum ferrofluid*. Nature **530,** 194–197 (2016).

[13] Petrov, D. S. *Quantum Mechanical Stabilization of a Collapsing Bose-Bose Mixture*. Phys. Rev. Lett. **115,** 155302 (2015).

[14] Chandler, D., Weeks, J. D. & Andersen, H. C. *Van der Waals Picture of Liquids, Solids, and Phase Transformations*. Science **220,** 787–794 (1983).

[15] Lee, T. D., Huang, K. & Yang, C. N. *Eigenvalues and eigenfunctions of a Bose system of hard spheres and its low-temperature properties*. Phys. Rev. **106,** 1135–1145 (1957).

[16] Roberts, J. L. *et al. Controlled Collapse of a Bose-Einstein Condensate*. Phys. Rev. Lett. **86,** 4211–4214 (2001).

[17] Cabrera, C. R. *et al. Quantum liquid droplets in a mixture of bose-Einstein condensates*. Science **359,** 301–304 (2018).

[18] Chomaz, L. *et al. Quantum-Fluctuation-Driven Crossover from a Dilute Bose- Einstein Condensate to a Macrodroplet in a Dipolar Quantum Fluid*. Phys. Rev. X **6,** 041039 (2016).

[19] Petrov, D. S. & Astrakharchik, G. E. *Ultradilute Low-Dimensional Liquids*. Phys. Rev. Lett. **117,** 100401 (2016).

[20] Boudjemâa, A. *Two-dimensional quantum droplets in dipolar Bose gases*. New Journal of Physics **21,** 093027 (2019).

[21] Morera, I., Astrakharchik, G. E., Polls, A. & Juliá-Díaz, B. *Universal Dimerized Quantum Droplets in a One-Dimensional Lattice*. Phys. Rev. Lett. **126,** 023001 (2021).

[22] Tylutki, M., Astrakharchik, G. E., Malomed, B. A. & Petrov, D. S. *Collective excitations of a one-dimensional quantum droplet*. Phys. Rev. A **101,** 051601 (2020).

[23] Łebek, M. *Elementary excitations of one-dimensional dipolar quantum Bose droplets*. MSc thesis (Uniwersytet Warszawski, Wydział Fizyki, 2021).

[24] Ołdziejewski, R., Górecki, W., Pawłowski, K. & Rzążewski, K. *Strongly Correlated Quantum Droplets in Quasi-1D Dipolar Bose Gas*. Phys. Rev. Lett. **124,** 090401 (2020).

[25] Białynicki-Birula I., M. C. & Kamiński, J. *Theory of Quanta* (Oxford University Press, New York, 1992).

[26] Damski, B. *Formation of shock waves in a Bose-Einstein condensate*. Phys. Rev. A **69,** 043610 (2004).

[27] Peotta, S. & Ventra, M. D. *Quantum shock waves and population inversion in collisions of ultracold atomic clouds*. Phys. Rev. A **89,** 013621 (2014).

[28] Choi, S., Dunjko, V., Zhang, Z. D. & Olshanii, M. *Monopole Excitations of a Harmonically Trapped One-Dimensional Bose Gas from the Ideal Gas to the Tonks-Girardeau Regime*. Phys. Rev. Lett. **115,** 115302 (2015).

[29] Lieb, E. H. & Liniger, W. *Exact analysis of an interacting bose gas. I. the general solution and the ground state*. Phys. Rev. **130,** 1605–1616 (1963).

[30] Lieb, E. H. *Exact analysis of an interacting bose gas. II. the excitation spectrum*. Phys. Rev. **130,** 1616–1624 (1963).

[31] Dalfovo, F., Giorgini, S., Pitaevskii, L. P. & Stringari, S. *Theory of Bose-Einstein condensation in trapped gases*. Rev. Mod. Phys. **71,** 463 (1999).

[32] Castin, Y. *Bose-Einstein Condensates in Atomic Gases: Simple Theoretical Results*. Coherent atomic matter waves, 1–136.

[33] Pitaevskii, L. P. & Stringari, S. *Bose-Einstein Condensation* (Clarendon Press, 2003).

[34] Lopes, R. *et al.* *Quantum Depletion of a Homogeneous Bose-Einstein Condensate*. Phys. Rev. Lett. **119,** 190404 (2017).

[35] Chang, R. *et al.* *Momentum-Resolved Observation of Thermal and Quantum Depletion in a Bose Gas*. Phys. Rev. Lett. **117,** 235303 (2016).

[36] Lang, G., Hekking, F. & Minguzzi, A. *Ground-state energy and excitation spectrum of the Lieb-Liniger model : accurate analytical results and conjectures about the exact solution*. SciPost Phys. **3,** 003 (2017).

[37] Girardeau, M. *Relationship between Systems of Impenetrable Bosons and Fermions in One Dimension*. J. Math. Phys. **1,** 516 (2004).

[38] Mancarella, F., Mussardo, G. & Trombettoni, A. *Energy–pressure relation for low-dimensional gases*. Nuclear Physics B **887,** 216–245 (2014).

[39] Dunjko, V., Lorent, V. & Olshanii, M. *Bosons in Cigar-Shaped Traps: Thomas-Fermi Regime, Tonks-Girardeau Regime, and In Between*. Phys. Rev. Lett. **86,** 5413 (2001).

[40] Kolomeisky, E. B., Newman, T. J., Straley, J. P. & Qi, X. *Low-Dimensional Bose Liquids: Beyond the Gross-Pitaevskii Approximation*. Phys. Rev. Lett. **85,** 1146 (2000).

[41] Kopyciński, J. *et al. Beyond Gross-Pitaevskii equation for 1D gas: quasiparticles and solitons*. SciPost Phys. **12,** 23 (2022).

[42] Jackson, J. D. *Classical Electrodynamics* (John Wiley and Sons, New York, 1999).

[43] Deuretzbacher, F., Cremon, J. C. & Reimann, S. M. *Ground-state properties of few dipolar bosons in a quasi-one-dimensional harmonic trap*. Phys. Rev. A **81,** 063616 (2010).

[44] McArdle, S. *et al. Variational ansatz- based quantum simulation of imaginary time evolution*. npj Quantum Information **5** (2019).

[45] Huang, K. *Podstawy fizyki statystycznej* (Wydawnictwo Naukowe PWN, Warszawa, 2006).

[46] Idziaszek, Z. *Kwantowe fluktuacje zimnych gazów atomowych*. PhD thesis (Centrum Fizyki Teoretycznej Polskiej Akademii Nauk, 2001).

[47] Politzer, H. D. *Condensate fluctuations of a trapped, ideal Bose gas*. Physical Review A **54,** 5048–5054 (1996).

[48] Byron, F. W. & Fuller, R. W. *Matematyka w fizyce klasycznej i kwantowej* (Wydawnictwo Naukowe PWN, Warszawa, 1974).

[49] Ensher, J. R., Jin, D. S., Matthews, M. R., Wieman, C. E. & Cornell, E. A. *Bose-Einstein Condensation in a Dilute Gas: Measurement of Energy and Ground-State Occupation*. Phys. Rev. Lett. **77,** 4984–4987 (1996).

[50] Lima, A. R. P. & Pelster, A. *Beyond mean-field low-lying excitations of dipolar Bose gases*. Phys. Rev. A **86,** 063609 (2012).